國立臺灣大學生命科學院植物科學研究所

博士論文

Institute of Plant Biology
College of Life Science
National Taiwan University
Doctoral Dissertation

不同阿拉伯芥銅鋅超氧歧化酶對其活化機制偏好之研究

Copper Chaperone-Dependent and -Independent Activation of Three Copper-Zinc Superoxide Dismutase Homologs Localized in Different Cellular Compartments in *Arabidopsis*

黃建勛

Chien-Hsun Huang

指導教授：靳宗洛 博士

Tsung-Luo Jinn, Ph.D.

中華民國 101 年 3 月

致謝

CCS-independent pathway 的發表，就結果來說並不驚人，但其過程對我來說卻是一段曲折迂迴、感觸良深的故事：

從碩班開始，我就對 SOD 的議題充滿興趣，只是當時朱瓊枝學姊的論文發表不久，實驗剛好告了一個段落，並不清楚未來研究方向的潛力，因此便與文鈺兩人朦朦懂懂的胡亂摸索，我本人除了 CuZnSOD 的相關研究，還同時做過 MnSOD、葉形突變株、蕃茄耐熱開花系統等研究，當時與文鈺懷抱著極大熱情，不分假日晝夜全心投入於實驗中，同時投資許多不同議題的研究，就是希望哪一個議題能首先出現有發表價值的結果，當時比較領先的研究其實是 MnSOD 的部分，然而就在直昇博班沒多久，MnSOD 的議題就被別人搶先發表了，當時受到不小的打擊，心灰意冷、茫然不知所措之下，決定先去當兵離開想想。這段時間，有賴文鈺對 CuZnSOD 的議題以酵母菌異位表現的方式繼續研究，結束兵役回來，感到這些進展是有發表價值的，因此日後就完全集中在 CuZnSOD 的研究上。只是後續的研究並不如想像中的順利，先是發現原來前人認為的三個 CuZnSOD 的活性 band 是錯誤的，再發現植物體內的 SOD 活性強弱與性狀並無關聯，加上 GSH 參與的不確定性，諸如此類在其他物種未見，與現有發表知識產生極大衝突、難以解釋的結論，導致我們的研究結果很難被其他 reviewer 接受，時常多所質疑與否定，因此，前前後後共投了 7 次，其中有許多不足為外人所道的辛酸。直至同樣矛盾的現象也陸陸續續的被其他研究室所揭露，才開啟了他人正視我們研究成果的契機。

這段時間，真的要非常感謝靳宗洛老師對我們的支持，從實驗開始，老師就大膽的放手讓我們自己去嘗試，其中因為經驗不足，或是嘗試一些異想天開的奇思妙想，免不了浪費不少實驗室的經費，而在 paper 屢投不上、被別人批評的一文不值的時候，也真的很感謝老師仍然相信並且肯定我們的價值，使我們在萬般沮喪之中，仍然存有信心繼續嘗試，努力突破，也才能有今天的成果，所以在此真的要說：『老師，謝謝你！』；此外，文鈺一路走來都是一同並肩作戰的伙伴，實驗時互相爭論思考，沮喪失意時互相扶持，每一道難關都有文鈺協同的足跡，因此沒有文鈺可能就沒有這篇論文的存在，只是在我因為這篇 paper 而達成了畢業標準的時候，文鈺 FeSOD 的 paper 還在 reviewer 熊熊砲火的攻擊之下，致使我們無法一起畢業，一同享受成功的喜悅，實在深感遺憾。在此要說：『女王，真的謝謝你，加油！』；至於在我們困苦的時候，給予安慰、建議、打氣的諸多老師及同學，建勛在此表達誠摯的感謝之意，也希望大家都能身體健康，萬事如意！

人生的許多苦難磨練著我們，在失意之中我們往往怨懟惱怒、傷心委屈，只是儘管如此，我們必須學會放下怨恨，才能懷抱希望；必須撫平傷痛，才能興起感激。痛苦是會過去的，成功也不是永恆的，因此只願我們一路行來，能夠忘卻曾經的不如意，只記得美好的部分，在愛與被愛之中，滿懷感恩的待人處世，慈憂眾生。

在此以一首詩，作為這段日子的紀念：

總有一些光
會抵達明日的居所
比鳥雀比黎明
依稀更早

總有一些光
會寫信給昨天的暗影
在透明的窗前
留下枝椏扶疏的日記

在天明時刻
鐵鳥斂著羽翅
思索海的句子
事物因此柔軟
有了陰影

雲朵吹開了黑暗
不需拆卸不需抵擋
總有一些殘瓦
會被顫抖的光陰擊中
落入雪中深埋

這是冬天也不是冬天
那裡有一顆晨星
帶著亡逝的荒塚與愛
迴蕩在廢棄的昨日
在躍動的海洋

櫻花木悄悄然的盛開了
即使沒有樹葉也揚起了風帆

TABLE of CONTENTS

摘要

超氧歧化酶(Superoxide Dismutase；SOD)，可將超氧分子轉變為過氧化氫及氧分子，具有解除氧化逆境的功能。對於銅鋅超氧歧化酶(CuZnSOD；CSD)的活化機制，目前已知有兩條路徑，一者是藉由銅鑲嵌輔助蛋白(Copper Chaperone of SOD1；CCS)的幫助，達到銅離子鑲嵌與形成內生性雙硫鍵的活化型態；另一者則是在人類及老鼠中發現，在沒有CCS情況下，CuZnSOD仍然具有少量的活性，只是其活化途徑與機制仍未明朗。本論文，將阿拉伯芥三個不同的CuZnSOD基因表現於酵母菌及阿拉伯芥原生質體中，我們證實阿拉伯芥不同CuZnSOD的活化具有不同的偏好：CSD1 位在細胞質中，可藉由兩條活化機制達成活化，在無CCS的情況下，仍保有~36%的活性，類似人類的CuZnSOD；CSD2 位在葉綠體中，只能經由CCS來達成活化，與酵母菌的CuZnSOD類似；CSD3 位在過氧化體中，只經由非CCS的路徑來達成活化，類似線蟲的CuZnSOD。我們證實在*AtCCS*-knockout突變株中，此殘存的CuZnSOD活性量就足以提供正常生理功能之所需。最後，我們也證實了還原態的穀胱甘肽(Glutathione；GSH)參與在非CCS的活化CuZnSOD的路徑上，並且需有一未知功能的因子共同合作才能完成。我們綜合前人之研究及本實驗之證據，提出兩種不需經由CCS而達成活化的可能作用機制，以及提出CuZnSOD蛋白質之C端具有與未知因子交互作用，而達成促進活化的功用。綜上而言，我們的研究提出植物體之複雜精密的抗氧化途徑，是在其他物種中從所未見的，而其詳細的機制，則仍有待後續的研究加以釐清。

ABSTRACT

Superoxide dismutases (SODs) are enzymes that protect cells from oxidative damage. The major pathway for CuZnSOD activation involves the function of a Copper Chaperone for SOD (CCS), whereas an additional, minor CCS-independent pathway that has been observed in mammals. Through overexpression of three *Arabidopsis* CuZnSOD genes (CSDs) in yeast and *Arabidopsis* protoplasts, we demonstrate the existence of a CCS-independent activation pathway in *Arabidopsis thaliana*. Interestingly, the three *Arabidopsis* CSDs show strongly different preference for the two activation pathways: the main activation pathway for CSD1 in the cytoplasm involved a CCS-dependent and -independent pathway, which was similar to that for human CSD. Activation of CSD2 in chloroplasts depended totally on CCS similar to yeast (*Saccharomyces cerevisiae*) CSD. Peroxisome-localized CSD3 via a CCS-independent pathway was similar to nematode (*Caenorhabditis elegans*) CSD in retaining activity in the absence of CCS. The residual SOD activity detected in AtCCS knockout plants is sufficient for seed germination and root growth, confirming that this alternative pathway is physiologically functional. Through a series of glutathione manipulation experiments, we further confirmed that glutathione plays a role in CCS-independnet pathway but must cooperate with an unknown factor for SOD activation. According to previous publications and our finding, two models of the CCS-independent mechanism are proposed. We also suggest that the CSD protein conformation at C-terminal is

important in providing a docking site for unknown factor to interact with. Our findings reveal a complex system underlying CSD activation which ensures a highly specific and sophisticated regulation of antioxidant pathways in plants and has not been reported in other organisms. However, the clear and definite mechanism needs further investigation.

ABBREVIATIONS

BH : *tert*-butyl hydroperoxide

BSO: L-buthionine sulfoximine

CCS: copper chaperone for superoxide dismutase

CDNB: 1-chloro-2,4-dinitrobenzene

CSD: the innate *Arabidopsis* copper/zinc superoxide dismutase

CuZnSOD: copper/zinc superoxide dismutase

FeSOD: iron superoxide dismutase

GFP: green fluorescence protein

MV: methyl viologen

MnSOD: manganese superoxide dismutase

NiSOD: nickel superoxide dismutase

ROS: reactive oxygen species

RT-PCR: reverse transcription-polymerase chain reaction

SOD: superoxide dismutase

TEMED: N,N,N',N'–tetramethyl-ethylenediamine

INTRODUCTION

Reactive oxygen species (ROS) are detrimental byproducts of aerobic reactions such as respiration and photosynthesis that can cause severe damage to numerous cellular constituents. Superoxide dismutases (SODs) are a group of metalloenzymes that defend against free radical species by disproportionating O_2^- into H_2O_2 and O_2 molecules (Beyer et al., 1991; Bowler et al., 1992).

Superoxide Dismutases: Classification and Localization

By a specific metal cofactor required for the superoxide scavenging activity (McCord and Fridovich, 1969), SODs are classified as Cu-Zn SOD (CuZnSOD), Fe SOD (FeSOD), Mn SOD (MnSOD) or Ni SOD (NiSOD) (Alscher et al., 2002; Zelko et al., 2002). Most eukaryotic cells contain more than 2 types of SODs, with CuZnSOD usually located in the cytoplasm, chloroplast, and probably extracellular space (Crapo et al., 1992); MnSOD located in mitochondria and peroxisome (Weisiger and Fridovich, 1973; Marres et. al., 1985); FeSOD located in chloroplast. However, FeSOD can only be found in prokaryotes and plants but not in animals (Alscher et al., 2002).

In *Arabidopsis thaliana*, seven SOD genes have been identified (Kliebenstein et al., 1998). FeSODs are located in the chloroplast, MnSODs in the mitochondrion, and CuZnSOD exists as

numerous isoforms that are distributed among various subcellular compartments (Jackson et al., 1978; Kanematsu and Asada, 1989; Bowler et al., 1992; Bueno et al., 1995). There are three CuZnSOD (CSD) genes: CSD1 which localizes to the cytoplasm, CSD2 which is found in chloroplasts, and CSD3 which is presumed to localize in peroxisomes (Kliebenstein et al., 1998; Alscher et al., 2002). Because phospholipid membranes are impermeable to O_2^- (Takahashi and Asada, 1983), protection of different organelles can be achieved by the distribution of SOD to different cellular compartments. In green tissue, the greatest protein accumulation and activity are found for CSD1, CSD2, MSD1, and FSD1 in *Arabidopsis* (Kliebenstein et al., 1998).

Evolution of Different Types of SODs

This cladogram containing the protein sequences of all seven *Arabidopsis* SODs, and the protein sequences of SODs from a variety of other plant species, clearly supports the suggestion that the FeSODs are of greatest antiquity and that the CuZnSODs evolved independently of the Fe and MnSODs (Alscher et al., 2002). It implies that MnSOD and FeSOD are more ancient types, and these enzymes very probably have arisen from the same ancestral enzyme, whereas CuZnSODs have no similarity to MnSOD and FeSOD in sequence and probably have evolved separately in eukaryotes (Kanematsu and Asada, 1990; Smith and Doolittle, 1992).

Such evolution is probably related to the varied availability of soluble transition metal

compounds in the biosphere, which was due to the O_2 content of the atmosphere in different geological eras (Bannister et al., 1991).When the atmosphere was fully replenished with oxygen, Fe (II) was almost fully unavailable whereas insoluble Cu (I) was converted into soluble Cu (II). At this stage, Cu (II) began to be used as the cofactor at the active sites of SODs. Transition from the use of iron to manganese only required little change in SOD protein structure since FeSODs and MnSOD show similar electrical properties. Thus, structures of MnSOD and FeSOD are very similar. However, the electrical properties of CuZnSOD are greatly different from those of FeSOD and MnSOD. After Cu becoming a metal cofactor, a major change should occur in the structure of the protein (Bannister et al., 1991). Nowadays, CuZnSODs have been found mostly in eukaryotes while FeSOD and MnSOD are present both in prokaryotic and in eukaryotic organisms. However, CuZnSODs have been observed in some bacteria, including *Caulobacter crescentus*, *Photobacterium leiognathi*, and pseudomonads. Three hypotheses might explain the presence of CuZnSOD in prokaryotes: (1) CuZnSODs in prokaryotes and eukaryotes evolved independently; (2) Gene of CuZnSOD originated in the eukaryotes and was transferred into the prokaryotes. (3) CuZnSOD originated in prokaryotes, and then the prokaryotic gene was transferred to eukaryotes. The third hypothesis depends on the unlikely requirement that prokaryotic and eukaryotic enzymes have a common ancestor that had CuZnSODs before the time that prokaryotes and eukaryotes separated. For the second hypothesis, it was first proposed by Martin and Fridovich (Martin and

Fridovich, 1981) and was support from Bannister and Parker (Bannister and Parker, 1985) by the reason of the 30% similarity between the protein sequences of the CuZnSODs in ponyfish and in its symbiont Photobacterium leiognathi. This similarity increased to 44% after taking point mutations into consideration, bringing more support to the hypothesis (Leunissen and de Jong, 1986). However, the presence of CuZnSOD in *Caulobacter crescentus* and in pseudomonads that are not symbionts suggests the hypothesis requires further refinement (Steinman, 1982; Steinman, 1985).

Regulation of SODs Expressions by Their Promoter Sequences

The promoter sequences of SODs were related to the regulation of gene expression under different stresses. Four consensus sequences were revealed to have the ability to bind to four different transcription factors, respectively (Alscher et al., 2002). (1) The ABA responsive element (ABRE) appears to be associated with genes responding to osmotic stress (high osmoticum, salt, desiccation, and cold) and binds to several similar sequences of eight nucleotides (Choi et al., 2000; Guan and Scandalios, 1998); the consensus sequence YACGTGGC was used. (2) NF-κB is a transcription factor that activates immunoglobulin-κ genes; the consensus sequence GGRNNYYCC was used (Smith et al., 2000). (3) The heat shock protein gene promoter consensus sequence is the palindromic sequence TTCNNGAA (Santos et al., 1996). (4) the Y-box motif has consensus sequence GATTGG and mediates redox-dependent transcription activation (Guan and Scandalios,

1998). In Table 1, diamonds (◆) summarize the exact or close matches found at upstream locations (within 1000 nucleotides of the ATG where transcription begins). The consensus sequences analysis revealed that different SODs may express under different stresses, which indicate they may have different roles in *Arabidopsis*.

Copper-Zinc SOD

CuZnSOD is a homodimeric copper- and zinc-containing enzyme (McCord and Fridovich, 1969). Zinc is required for the structural integrity of the protein and influences enzyme activity, whereas copper plays a catalytic role in the disproportion of superoxide (Forman and Fridovich, 1973; Beem et al., 1974). The acquirement of both metal ions was first assumed to be by passive diffusion; however, Rae et al. (1999) found that the intracellular concentration of free copper is undetectable under normal physiological conditions, which suggests that cells require copper chaperones to facilitate copper transfer to specific partners (see below).

CuZnSODs are found throughout the plant cell. There are two different groups of CuZnSODs, which are homodimeric and homotetrameric (Bordo et al., 1994). The active sites of each subunit function independently. When these subunits are separated and coupled with an inactive subunit, newly formed enzymes show full activity, which provides evidence that the interactions between the subunits are not essential for full catalytic activity (Fridovich, 1986).

There are chloroplastic and cytosolic forms of CuZnSOD. Deduced amino acid sequences of these two isoforms show approximately 68% similarity, whereas there is approximately 90% similarity among the chloroplastic CuZnSODs (CuZnSODchl) and 80–90% similarity among the cytosolic CuZnSODs (CuZnSODcyt). The occurrence of a peroxisomal CuZnSOD from watermelon was also previously reported, which represented about 18% of the total SOD activity in the cell (Sandalio and del Río, 1987). Presence of such a peroxisomal CuZnSOD also was shown in rat liver cells (Dhaunsi et al., 1992).

Arabidopsis CuZnSODs are regulated by Copper-regulated miR398

A microRNA, miR398, is shown to regulate CSD1 and CSD2, targeting CSD1 and CSD2 mRNA for degradation during growth on low Cu condition (Sunkar et al., 2006; Yamasaki et al., 2007; Dugas and Bartel, 2008). miR398 is one of several Cu-regulated microRNAs (the Cu-microRNAs) that down-regulate transcripts for a number of Cu proteins together during Cu-limited growth (Abdel-Ghany and Pilon, 2008). The Cu-microRNAs are regulated by a transcription factor called SPL7 (Yamasaki et al., 2009), a homolog of Chlamydomonas rheinhardtii CRR1, which is possibly a Cu-sensing protein (Kropat et al., 2005). It was proposed that the mechanism of Cu-protein down-regulation during Cu-limited condition allows for preferential delivery of Cu to plastocyanin (Burkhead et al., 2009), which is essential for electron transport and

survival of higher plant (Weigel et al., 2003)

SOD Activation Requires a Metallochaperone

The metal cofactors for SODs are transition metals, whose ability to readily accept or donate an electron are utilized in the superoxide dismutation process. In free form, however, these metal ions produce potentially harmful hydroxyl radicals via the Haber-Weiss reaction (Halliwell and Gutteridge, 1989). Hence, it is generally accepted that free transition metals must exist in a complexed form and that SOD activation should require a metallochaperone. It has also been reported that in spite of the high affinity of SOD1 for copper (dissociation constant = 6 fM) and the high intracellular concentrations of both SOD1 (10 μM in yeast) and copper (70 μM in yeast), the copper chaperone for the superoxide dismutase (CCS) gene is still necessary for expression of an active, copper-bound form of superoxide dismutase (SOD1) in vivo (Rae et al., 1999).

Previous Studies on the Function of CCS

The first metallochaperone to be identified was the copper chaperone for SOD1 (CCS) in yeast Saccharomyces cerevisiae (yCCS) (Culotta et al., 1997). Orthologs of this protein have been found in many species (Abdel-Ghany et al., 2005; Chu et al., 2005). It is known that CCS consists of three protein domains (I, II, and III). The central domain II resembles SOD1 and serves to dock CCS with

SOD1 (Schmidt et al., 1999). Once the CCS-SOD1 heterodimer formed, copper insertion and disulfide oxidation may proceed via a CXC copper-binding motif at the C-terminal CCS domain III. In the CCS-SOD1 docked complex structure, CCS domain III Cys229 forms an intermolecular disulfide with Cys57 of SOD1, which is believed to represent the intermediate in forming the SOD1 intramolecular disulfide. Domain I harbors a single CXXC copper-binding motif, it may help CCS dock with an upstream source of copper. To sum up, CCS protein physically interacts with CuZnSOD, thereby assisting in copper incorporation and the catalysis of disulfide bond formation, and thus resulting in an active SOD (Casareno et al., 1998; Lamb et al., 2001; Brown et al., 2004; Furukawa et al., 2004).

Discovery of *Arabidopsis* CCS

In *Arabidopsis*, Pilon et al. (2005) has reported that AtCCS is a functional homolog of the yeast copper chaperone Ccs1/Lys7. After that, Chu et al. (2005) also found that a single CCS (AtCCS) is capable of activating three CSDs in different compartments. Nevertheless, the phenotype of a CCS-knockout mutant (*Atccs*) has been found to be normal (Cohu et al., 2009). These data indicate the existence of additional activating factors for CSDs.

CCS-Independent Activation of CuZnSOD

A CCS-independent activation pathway for CuZnSOD had been observed in mice and further studied in a yeast expression system (Wong et al., 2000; Subramaniam et al., 2002; Carroll et al., 2004). To date, yeast SOD1 (ySOD1) activation has been found to fully depend on yeast CCS (yCCS; Carroll et al., 2004), whereas the nematode (*Caenorhabditis elegans*) CSD (wSod-1) is exclusively activated independently of CCS (Jensen and Culotta, 2005). Human CSD (hSOD1) is largely activated by CCS but retains about 25% to 50% of its activity in the absence of CCS (Carroll et al., 2004). However, CCS-independent pathways for SOD activation in plants are not well understood

Reduced glutathione (GSH) was required for CCS-independent activation of hSOD1 in yeast CCS-mutant strains with defective GSH metabolism, and wSod-1 was inactive in the presence of CCS when GSH was depleted in yeast (Carroll et al., 2004; Jensen and Culotta, 2005). However, a direct interaction between GSH and CSD has yet to be demonstrated. Results from mutagenesis studies showed that amino acid residues 142 and 144 near the carboxyl terminus of human and yeast CSDs were important in the CCS-independent pathway (Carroll et al., 2004; Jensen and Culotta, 2005). When these residues were replaced by those of dual prolines in ySOD1, CCS-independent activities for both hSOD1 and wSod-1 were inhibited. A recent study further confirmed that the proline at residue 144 but not 142 restricted ySOD1 disulfide formation in the absence of CCS, which played a key role in blocking CCS-independent activation (Leitch et al.,

2009a).

Besides, it has demonstrated that CCS activation of SOD1 requires molecular oxygen, whereas there is no similar oxygen dependence with CCS-independent activation (O'Halloran et al., 2004). Hence, CCS-independent activation allows SOD1 activity to be maintained over a range of oxygen conditions. This can be particularly critical in tissues of multicellular organisms where oxygen tensions range from near atmospheric to hypoxic.

Aims of the Dissertation

In our current study, we analyzed *Arabidopsis* and yeast knockout strains to investigate the dependence of *Arabidopsis* CSD activity on CCS metallochaperone. We found both CCS-dependent and -independent activation pathways are present in *Arabidopsis*, and three *Arabidopsis* CSD proteins display unique levels of dependence on each of the two activation pathways. Moreover, we show that the chloroplast is unique in having lost CCS-independent activation ability. This phenomenon represents a novel finding as it has not been reported for any other species. We also suggest from our current data that glutathione is involved in the CCS-independent pathway in *Arabidopsis*, with an additional factor cooperatively assisting in CSD activation

MATERIALS AND METHODS

Plants, Yeast Strains, Media and Growth Conditions

The *Arabidopsis thaliana Atccs* (At1g12520) and *Atcsd1* (At1g08830) knockout lines of Columbia ecotype, *Atccs* (SALK_025986) and *Atcsd1* (SALK_109389), were obtained from the ABRC (Ohio State University, USA) (Chu et al., 2005). Seeds were incubated at 4°C for 4 d in the dark before sowing, and then plants were grown in a growth chamber under 16-h light/8-h dark at 21 to 23°C at a light intensity of 60 to 100 μmol m^{-2} s^{-1}. *Saccharomyces cerevisiae* BY4741 (*MAT***a**, *his3Δ1*, *leu2Δ0*, *met15Δ0*, *ura3Δ0*) was used as the yeast wild type (WT); *sod1*Δ (*sod1*::*kanMX4*) and *ccs*Δ (*ccs*::*kanMX4*) are derivatives of BY4741. Enriched yeast extract, peptone-based medium supplemented with 2% (w/v) Glc (YPD), and synthetic dropout leucine medium was used to propagate the yeast strains. Yeast was incubated at 30°C under aerobic conditions without shaking, and G418 was used at 200 μg mL^{-1} to maintain the *ySOD1* and *yCCS* deletions in the yeast as required.

Protein Extraction, In-gel SOD Activity Assay and Immunoblotting

Arabidopsis crude protein was extracted with 150 mM Tris, pH7.2, as described previously (Chu et al., 2005). Yeast crude protein was extracted by the glass bead lysis protocol according to Culotta et al. (1997). Protein concentration was determined by the Bradford method (1976) with the

Bio-Rad protein assay reagent (Bio-Rad, CA, USA). In-gel SOD activity assay and immunoblotting were performed on 10% to 15% (w/v) nondenaturing or denaturing gels, respectively, according to Chu et al. (2005). The SOD activities and protein signals were quantified by analyzing the activity gels and immunoblotting membranes with LAS-3000 (Fuji Film, Tokyo, Japan) and ImageQuant software (Molecular Dynamics, CA, USA).

RNA Extraction, RT-PCR and Gene Cloning

Total RNA was prepared with TRIZOL reagent (Invitrogen, CA, USA) and TURBO DNA-*free* Kit (Applied Biosystems, CA, USA). cDNA synthesis was performed by using high-capacity cDNA Reverse Transcription Kits (Applied Biosystems). RT-PCR and gene cloning was performed with the primers described in Supplemental Table 2 online.

Constructs

All cDNA fragments were amplified with PCR and then cloned at yT&A vector (Yeastern Biotech, Taipei, Taiwan); subsequent construction was performed after DNA sequencing. For constructs used in yeast expression, all genes from ATG to stop codon were inserted at the *Hind*III site of the 2 μ *LUE2* yeast shuttle vector pADNS (Colicelli et al., 1989), with the exception of CSD3, which was inserted at the *Not*I site. Point mutations of CSD1 were created by the

megaprining method with the primers described in Supplemental Table 2 online. For GFP and YFP fusion constructs, 326-GFPnt vector (Lee et al., 2001) and p35S-EYFP vector (see below) were used, respectively. For overexpression in protoplasts, genes were also subcloned into p35S-EYFP vector with a stop codon. A double 35S promoter from pPE1000 vector (Hancock et al., 1997) was cloned into the *Xho*I/*Hind*III sites of pEYFP vector (Clontech, CA, USA), and the CSD1, CSD2 and CSD3 genes were then cloned into this p35S-EYFP vector at the *EcoR*I/*BamH*I, *Hind*III, and *EcoR*I sites, respectively. For ΔTP-CSD2, the 61 amino acids at the C terminus were deleted by using the primer described in Supplemental Table 2 online, and then inserted into p35S-EYFP at *Hind*III site. Transit peptide of CSD2 was amplified using the primer described in Supplemental Table 2 online. Then, TP_{CSD2} with *EcoR*I/*Nco*I sites, and CSD1 gene with *Nco*I/*Sal*I sites, were ligated into p35S-EYFP at *Eco*I/*Sal*I sites. For GFP fusion, CSD3 and CSD3-dAKL was inserted into 326-GFPnt vector at *Sma*I/*Sal*I site. Both ROXY1 and GRXcp was inserted into *Sma*I/*BamH*I sites of p35S-EYFP with stop codon. For recombinant protein, CSD1 gene was inserted into pGEX-6P-1 (Amersham Pharmacia Biotech) at *EcoR*I site.

Treatments for Seed Germination Rate

Sterilized seeds of the WT, *Atccs* and *Atcsd1* were plated on 1/2 MS medium supplemented with 1% (w/v) Suc and pretreated with 4°C in the dark for 3 d. Seeds were then incubated at 23°C

under 16-h light/8-h dark for 3 d, and seed germination rate was observed. Methyl viologen (MV; Sigma, MO, USA) and *tert*-butyl hydroperoxide (BH; Fluka Chemical Co., WI, USA) was added to the 1/2 MS plates at the indicated concentrations.

Monitoring Superoxide Anion Level by Nitroblue Tetrazolium

This assay was according to Myouga et al. (2008). Three-week-old plants grown on 1/2 MS medium supplemented with 1% (w/v) Suc were harvested, weighed and then infiltrated with 6 mM nitroblue tetrazolium (NBT) in 10 mM sodium phosphate buffer (pH 7.1) at 400 to 500 mbar for 15 min. Plants were then illuminated with 800 μmol m^{-2} s^{-1} for 1 h to produce color. Chlorophyll was removed by infiltration with ethanol/chloroform (4:1, v/v) at 400 to 500 mbar for 15 min for four times. Then, samples were solubilized in a mixture of 2 M KOH and DMSO at a ratio of 1:1.167 (v/v) and vortexed at 4°C for 1 h. After centrifugation at 13,000×*g* for 10 min, the NBT-formazan production was determined as the absorbance at 700 nm of the supernatant.

Treatments for Root Length Evaluation

Sterilized seeds of WT, *Atccs* and *Atcsd1* were plated on 1/2 MS medium supplemented with 1% (w/v) Suc, and pretreated with 4°C in the dark for 3 d. Plates were then incubated at 23°C for 3 d under continuous light condition for germination, and the seedlings were transferred to 1/2 MS

plates with each treatment and incubated at 23°C for another 4 d. After the root length was measured, the seedlings were collected to quantify the protein, total and reduced glutathione concentrations. Methyl viologen (paraquat, Sigma) and buthionine sulfoximine (BSO, Sigma) were added in the 1/2 MS plates at the indicated concentrations.

Lysine-Independent Aerobic Growth

Yeast strains were cultured in appropriate medium overnight at 30°C without shaking. Then, cells were centrifuged, washed and resuspended in sterile water, and the absorbance at 600 nm was measured. For plate assay, the yeasts were serial diluted from OD 600 = 1 to 10^{-4}, plated on synthetic dropout lysine medium, and incubated at 30°C under aerobic conditions for 3 d. Results in Figures 3 and 8 were performed on the same plate. For the liquid assay, the yeast cultures were seeded from OD 600 = 0.01 in the lysine-lacking medium, incubated at 30°C for 24 h under aerobic conditions, and then the cell density was determined by measuring the absorbance at 600 nm.

Protoplast Preparation and Transfection

Protoplast preparation and transfection were performed according to Yoo et al. (2007). The WT and *Atccs* plants grew on soil for 3 to 4 weeks, and the 5th to 8th leaves were chosen for protoplast preparation. About 10^6 protoplasts were transfected with 100 to 300 μg plasmid DNA for each

construct by the PEG-calcium method. After transfection, the cells were incubated in WI solution at room temperature for 16 h under continuous light conditions. For protein extract of protoplasts, cells were collected, resuspended in 150 mM Tris buffer (pH 7.2), and vortexed five times for 5 s. Cell lysate was then subjected to the SOD activity assay and immunoblotting.

Glutathione Treatment and Quantification

For treatments in yeast, L-buthionine sulfoximine (BSO; Sigma) was added to the medium at 1 mM for 16 h; 1-chloro-2,4-dinitrobenzene (CDNB, dissolved in 95% ethanol; Fluka) and reduced-form glutathione (GSH; Sigma) were added at 1 and 20 mM, respectively, for 2 h. Equal volumes of 95% ethanol or H_2O were added as mock treatments. *Atccs* flowers were detached and immersed in CDNB or GSH solutions at room temperature for 3 or 1 h, respectively. After CDNB or GSH solutions were removed, the flowers were washed with water 3 times and then the crude protein was extracted. For treatments of protoplasts, *Atccs* protoplasts transfected with CSD1 were first incubated at room temperature for 16 h for CSD1 protein expression, and then 1 mM GSH or CDNB was added into the incubation medium for 15 min. Total glutathione and GSH concentrations were quantified with use of the Total Glutathione Quantification Kit (Dojindo Laboratories, Kumamoto, Japan) and the QuantiChrom Glutathione Assay Kit (BioAssay Systems, CA, USA), respectively. The resulting concentrations were normalized to the protein concentration

of the same sample, and the values of glutathione concentration are expressed relative to those of the mock treatments.

Apo-CSD1 Protein Preparation and In Vitro Treatments

Recombinant GST fusion proteins were affinity purified according to the Glutathione-Agarose user manual (Sigma). The GST tag was removed by PreScission Protease (Sigma). For preparation of inactivated Apo-CSD1 (Lepock et al., 1981), Holo-CSD1 was dialyzed against buffer containing 50 mM sodium acetate (pH 4.0) and 10 mM EDTA at 4°C for 24 h, then against buffer containing 50 mM sodium acetate (pH 4.0) and 100 mM NaCl at 4°C for 24 h, and finally against buffer containing 50 mM potassium phosphate buffer (pH 7.8) at 4°C for 24 h. In the in vitro treatments, each reaction contained 870 ng Apo-CSD1 protein and 20 μM $ZnSO_2$ in PBS buffer (140 mM NaCl, 2.7 mM KCl, 10 mM Na_2HPO_4 and 1.8 mM KH_2PO_4, pH 7.3), and then 0.1 μM $CuSO_4$, 1 mM GSH or 15 μg *Atccs* cellular extract were added into the mixture as indicated. After incubation at room temperature for 30 min, 1.5 mM EDTA was added into samples, and then native-PAGE was performed with 0.1 mM EDTA in both the nondenaturing-gels and running buffer. In the treatments with both Cu and GSH, the two solutions were mixed and incubated at 4°C for 16 h before the experiment.

Antibodies

Anti-sera α-CSD1, α-CSD2 and α-CSD3 were generous gifts from Dr. D. J. Kliebenstein (Kliebenstein et al., 1998), and *Arabidopsis* α-RPN8 antibody was kindly provided by Dr. H.-Y. Fu (Yang et al., 2004). We also used antibodies of α-ACT (Chemicon, CA, USA), yeast α-PGK1 (Molecular Probes, OR, USA), anti-rabbit (Jackson ImmunoResearch, PA, USA) and anti-mouse IgG (Bethyl Laboratories, TX, USA) conjugated with alkaline phosphatase.

Statistical Analysis

All experiments were independently repeated at least three times. Statistical analysis was performed by using the Student's *t* test (two-tailed, unpaired).

Accession Number

Sequence data from this article can be found in GenBank as described in Table 1.

RESULTS

CSD Retains Partial Activity in the Absence of AtCCS in *Arabidopsis*

Previous studies have mapped the pattern of SOD activity among various *Arabidopsis* organs (Chu et al., 2005). The level of CSD activity was shown to be high in flowers and siliques but low in rosette leaves and cauline leaves. To determine whether *Arabidopsis* CSD can be activated in the absence of AtCCS, we analyzed CSD activities in the flowers of wild type (WT) and *Atccs* plants. As shown in Fig. 1, residual CSD activity (about 6% to 30% of the WT levels) could be clearly observed in the *Atccs* mutant (top), indicating that a CCS-independent CSD activation pathway exists in *Arabidopsis*. Also of interest was our observation that the CSD1 and CSD2 protein levels in *Atccs* were lower than those in the WT (Fig. 1, bottom), whereas their mRNA levels were shown previously to be equivalent (Chu et al., 2005). This may indicate that the activated CSD protein is more stable than its inactivated counterpart.

Activity Signals of CSD1 and CSD2 Are Partially Overlapped

In previous study, there are two major CSD activity bands in the *Arabidopsis* WT protein extracts. The slow migration band was previously characterized as CSD2, whereas the fast migration band was CSD1 (Chu et al., 2005). We again characterized the 3 CSD protein and activity in this research. In the denaturing gel, the 3 overexpressed CSD proteins signals can be clearly

identified by their size (Fig. 2A). However, transient overexpression of 3 CSDs in protoplasts revealed that one of the CSD2 activity bands overlapped with that of CSD1 (Fig. 2B, lanes 1 and 2). Thus, discriminating CSD1 and CSD2 activities by the in-gel SOD activity assay is difficult. Notably, the CSD3 protein signal was clear when overexpressed in protoplasts, but its activity was undetectable (Fig. 2B, lane 3). We also could not detect the endogenous CSD3 protein signal by α-CSD3 antibody in the WT tissues (data not shown), which indicated that the endogenous CSD3 expression level was too low to be detected. Therefore, we cannot identify which CuZnSOD can be activated by the CCS-independent pathway through a direct observation on the SOD activity signals; other experimental method must be taken.

CSD1 and CSD3 Show CCS-Independent Activities in Yeast

AtCCS is a functional homolog of yCCS (Abdel-Ghany et al., 2005), implying that the *Arabidopsis* CSD might be activated in a yeast system. As an additional method of determining which CSD can be activated via the CCS-independent pathway, we expressed the three *Arabidopsis* CSD genes in yeast SOD1- and CCS-knockout strains (referred to as *sod1*Δ and *ccs*Δ, respectively; Fig. 3). As revealed by the in-gel SOD activity assay (Fig. 3A, top), the CSD1 activity band was strong in *sod1*Δ and was weaker, but clearly visible, in *ccs*Δ (lanes 1 and 2), demonstrating a CCS-independent activation of CSD1. When CSD2 and CSD3 were overexpressed in yeast, no

detectable activity was observed (lanes 3 to 6), and the CSD2 protein was not detectable in either yeast line (Fig. 3A, lanes 3 and 4, bottom). Considering the limited sensitivity of the SOD activity and immunoblotting assays, we used lysine-independent aerobic growth as an indicator of the CSD activities in yeast in vivo because of its high sensitivity to SOD activity (Wallace et al., 2004). Using this assay, lysine biosynthesis ability is maintained when ySOD1 activity just higher than 2% of wild type activity (Corson et al., 1998). Because ySOD1 activation is fully dependent on yCCS function, the endogenous ySOD1 activity is lost in *ccs*Δ (Carroll et al., 2004), and the heterologous-expressed *Arabidopsis* CSDs should be exclusively responsible for the lysine biosynthesis ability in both *sod1*Δ and *ccs*Δ. In our experiments, both *sod1*Δ and *ccs*Δ were unable to grow under lysine-depleted conditions (Fig. 3B and 3C), which confirms the absence of ySOD1 activity in these two mutants. The lysine biosynthesis ability was recovered in both *sod1*Δ and *ccs*Δ upon CSD1 and CSD3 expression. Upon the expression of CSD2, the phenotype of *sod1*Δ was partially rescued but that of *ccs*Δ was not restored at all, thereby demonstrating a weak expression and activity of CSD2 in *sod1*Δ. CSD2 is a chloroplast protein in *Arabidopsis*; because of no chloroplasts in yeast, we wondered whether the transit peptide might cause misfolding of CSD2. Thus, we deleted the transit peptide of CSD2 (referred to as ΔTP-CSD2) and expressed it in yeast; however ΔTP-CSD2 still showed no activity in *ccs*Δ (Fig. 4). These results thus show clearly that CSD1 and CSD3 can both be activated via the CCS-independent pathway in yeast. However, the

failure of CSD2 to rescue lysine biosynthesis might be related to the heterologous nature of the expression system used. Thus, we sought additional means for determining whether CSD2 can be activated in a CCS-independent manner.

CSD2 Activation in Chloroplasts Requires CCS But Not in the Cytoplasm

To address the question of how CSD2 is activated, *CSD2* and *AtCCS* genes were transiently overexpressed in *Atccs* protoplasts (Fig. 5A and 5B). Use of yellow fluorescent protein (YFP) fused to CSD2 revealed that the full-length CSD2 localized in chloroplasts, whereas the transit peptide-deleted CSD2 (ΔTP-CSD2) localized to cytoplasm (Fig. 5A). Full-length CSD2 was activated in the presence of AtCCS (Fig. 5B, lane 2) but was undetectable in the absence of AtCCS (lane 3). However, ΔTP-CSD2 showed CCS-independent activity (lane 7), which indicates that CSD2 can be activated via the CCS-independent pathway when localized in cytoplasm.

CCS-Independent CSD1 Activation Occurs in the Cytoplasm but Not in Chloroplasts

To gain an understanding of CSD activation in chloroplasts, we constructed a chloroplast-directed CSD1 to observe its behavior in this compartment (Fig. 5C and 5D). We used YFP fusion proteins to confirm the localization of a CSD1 fused with the chloroplast transit peptide of CSD2 (TP_{CSD2}-CSD1) in chloroplasts (Fig. 5C). We found CCS-independent CSD1 activity in

Atccs (Fig. 5D), and the efficiency of CSD1 activation (activity μg^{-1} protein) in *Atccs* was ~36% of that in wild-type (compare lanes 2 and 3). In contrast, chloroplast-localized CSD1 was active in the presence of AtCCS (lane 6), and its activity was undetectable in the absence of AtCCS (lane 7). This result is consistent with the observation on CSD2 that CCS-independent CSD activation occurs in the cytoplasm but not in the chloroplast.

Activities of Both Peroxisomal and Cytoplasm-directed CSD3 Can Not Be Detected

A similar experiment was also performed with CSD3 (Fig. 6), and green fluorescent protein (GFP) fused to N-terminal of CSD3 to show its localization (panel A). Our result showed that CSD3 localized in peroxisomes as predicted, but its activity were undetectable even when it was overexpressed in *Atccs* with *AtCCS* co-expression (Fig. 6B). Deletion of the peroxisome-targeting sequence AKL at its C-terminal (CSD3-ΔAKL; Fig. 6A) leads to a cytoplasmic CSD3; however, unlike CSD1 and CSD2, there was still no activity detected (Fig. 6B).

Effect of Glutathione upon CCS-Independent CSD1 Activity in Yeast

Previous studies have implicated GSH in the CCS-independent activation of human hSOD1 (Carroll et al., 2004). To investigate the possible involvement of GSH in the activation of *Arabidopsis* CSD, we treated a yeast *ccs*Δ strain that expresses CSD1 with either GSH,

1-chloro-2,4-dinitrobenzene (CDNB, a glutathione chelator) or L-buthionine sulfoximine (BSO. a glutathione biosynthesis inhibitor), and then analyzed the effects upon CSD1 activities (Figure 7). When treated with CDNB, CDNB+BSO and BSO, the cellular concentrations of both total glutathione and GSH were significantly decreased to 0.68-, 0.36- and 0.6-fold, and 0.77-, 0.37- and 0.67-fold (Fig. 7A, treatments 2 to 4), respectively. The CSD1 activity was decreased to 0.4-, 0.52- and 0.83-fold respectively (Fig. 7B, lanes 2 to 4). Hence, decreased GSH levels correlate with a reduction in CCS-independent CSD activity. In addition, although the total glutathione and GSH concentrations were slightly enhanced upon GSH treatment by 1.6-fold and 1.33-fold (Fig. 7A, treatment 6), respectively, no corresponding increase in CSD1 activity was observed (Fig. 7B, lane 6).

Effect of Glutathione upon CCS-Independent CSD Activities in *Arabidopsis* Flowers

A similar experiment was performed using *Atccs* flowers, which were treated with either CDNB (a glutathione chelator) or GSH, and then analyzed for CSD activity (Fig. 8). Both total glutathione and GSH concentrations in *Atccs* flowers decreased significantly as a result of the CDNB treatment (Fig. 8A), and the corresponding CSD activity was strongly downregulated (Fig. 8C, lanes 1 to 4). Following GSH treatment, the total glutathione concentration greatly increased, whereas the GSH concentration increased only slightly (Fig. 8B). The relatively mild change

observed in the internal GSH concentration might be due to an in vivo mechanism that maintains the homeostasis of reducing power, too much of which could be potentially damaging to cells (Lockwood, 2003; Pasternak et al., 2008). Xiang et al. (2001) have also shown previously that the maximal enhancement of GSH was only 2-fold in a γ-glutamylcysteine synthetase overexpression line, similar to the 2-fold increase in GSH concentration observed in our present system (Fig. 8B). Although the bands were less well-defined, the major CSD activity band in the corresponding treatments seemed to show no enhancement (Fig. 8C, lanes 5 to 8, arrow).

Effect of Glutathione upon CCS-Independent CSD Activities in *Arabidopsis* Flower Protein Extract

An in vitro experiment was performed to further investigate the effect of GSH on CCS-independent CSD activities. By adding GSH directly into the *Atccs* flower protein extracts, CSD activities were quickly enhanced in 15-min incubation with 10 mM GSH treatment (Fig. 9A), but the enhancement was still within certain limit even with 20 mM GSH treatment for 1.5 h (Fig. 9B). The limitation of the GSH-dependent activation *in vitro* might be due to (1) the CSD activities activated by GSH are less efficient, and thus only weak activities could be present at one time; and (2) cellular proteins showed decreasing accumulation and/or stability in cells with abundant GSH (Fig. 9A and 9B, bottom panel; Lockwood, 2003), and the lowered CSD protein levels might result

in the weak enhancement.

Additionally, we also curious about that under normal condition, whether these two pathways each account for partial activation of CSD and thus have their own activation niche. To answer this, we treated WT flowers with CDNB to see the changes of CSD activities (Fig. 10). CDNB was added directly into the flower protein extract for efficient depletion of glutathione. In this *in vitro* test, the CSD activities showed no significant change either treated with different CDNB concentrations (5 to 20 mM; Fig. 10A) or with longer incubation time (from 15 to 90 minutes; Fig. 10B). Hence, the activation niche accounted by CCS-independent pathway seemed negligible in WT, which implied that CSD activation by AtCCS was so efficient that a decrease in glutathione level could be ignored.

Moreover, when we treated WT flower protein extracts with 10 mM GSH for 18 h, CSD1 protein was mostly degraded, whereas CSD2 protein was still preserved (Fig. 11); compared to CSD1, CSD2 was not sensitive to GSH, and thus the effect of GSH on CSD2 seemed not efficient.

Altering Glutathione Concentration by Drugs or Glutaredoxin Expression Affect CCS-Independent CSD Activities in *Arabidopsis* Protoplasts

The effects of GSH were also tested by altering its concentration in *Atccs* protoplasts transiently overexpressing CSD1 (Figure 12A). Cellular concentrations of total glutathione and

GSH were slightly enhanced upon GSH treatment by 1.23- and 1.13-fold, respectively, whereas the CSD1 activity levels showed no obvious increase in this system. Upon treatment with CDNB, both the concentrations of total glutathione and GSH decreased (to 0.42- and 0.87-fold), as did the amount of CSD1 and its level of activity.

In a further experiment, we manipulated the GSH concentration by overexpressing glutaredoxin, which oxidizes GSH to GSSG during its substrate-reducing reaction (Rouhier, 2010). To this end, we overexpressed ROXY1 (a cytoplasmic glutaredoxin) or GRXcp (a chloroplastic glutaredoxin) together with CSD1 in *Atccs* protoplasts (Figure 12B; Xing et al., 2005; Cheng et al., 2006; Rouhier, 2010). Our results revealed that the GSH concentration decreased as a result of either ROXY1 or GRXcp overexpression, whereas the total glutathione concentration showed no significant change (Figure 12B). When ROXY1 was co-expressed, both the amount of CSD1 as well as its activity level was diminished, whereas the co-expression of GRXcp resulted in reduced CSD1 activity with no change in the amount of protein.

Taken together, our results show an overall decrease in CSD1 activity upon reduction of the intracellular GSH concentration. However the decrease in GSH concentration is not well correlated with that of CSD1 activity. Additionally, no obvious change in CSD1 activity was observed when the GSH concentration was increased.

Activation of Apo-CSD1 by Cu and GSH is Greatly Enhanced When *Atccs* Cellular Extracts Is Added in Vitro

To gain a better understanding of GSH involvement in the CCS-independent pathway, we carried out in vitro analyses using purified recombinant proteins. We purified recombinant CSD1 protein as a GST fusion product (GST-CSD1), and then removed the GST tag by PreScission protease (generating Holo-CSD1). We then prepared inactivated Apo-CSD1 using an acid treatment method (Fig. 13A and 13B; Lepock et al., 1981). When Apo-CSD1 was treated with 0.1 μM Cu (Fig. 14, lane 2), CSD1 itself was able to spontaneously bind copper and recover its own activity. We then tested the effects of pH on this system (Fig. 13C), and found that the recovery of Apo-CSD1 activity was maximal at pH 7, the same pH used in our current experiments. Recovery of Apo-CSD1 activity was unsuccessful using 1 mM GSH alone, which was possibly due to the extremely low concentration of Cu in the mixture (Fig. 14, lane 3). However, treatment with both Cu and GSH did not result in greater CSD1 activity than treatment with Cu alone, indicating that GSH itself was either inefficient or possibly unable to facilitate CSD1 activation. When the same experiments were performed in the presence of *Atccs* cellular extracts (lanes 6 to 9), the activity of CSD1 treated with GSH/extract increased slightly (lane 8) as compared with a cellular extract treatment alone (lane 6). However, CSD1 activity was greatly enhanced when GSH, extract and Cu were present in the reaction mixture (lane 9), as compared with only Cu and extract (lane 7). This

indicates that GSH can activate CSD1 efficiently under these conditions. The fact that *Atccs* cellular extract can greatly affect the level of CSD1 activation by GSH indicates that the interaction between GSH and CSD1 is facilitated by a yet undetermined factor.

Superoxide Anion Level and Seed Germination Rate of WT, *Atccs* and *Atcsd1*

We endeavored to determine whether these residual CSD activities were physiologically functional in vivo by using the seed germination rate as a phenotypic indicator to compare WT, *Atccs* and CSD1 knockout lines (*Atcsd1*) after treatment with methyl viologen (MV) and *tert*-butyl hydroperoxide (BH). We used MV and BH to induce oxidative stress in cells and thereby magnify the phenotypic effects due to the defects in antioxidant enzymes such as SOD. In the homologous T-DNA-inserted *Atcsd1* knockout line, CSD1 mRNA and protein were absent, whereas the expression levels of CSD2 and CSD3 were unchanged (Fig. 15A to 15C). As visualized using an in-gel SOD activity assay, the total CSD activity in *Atcsd1* (with functional CSD2 and CSD3) was lower than that in the WT but was higher than that in *Atccs* (Fig. 15D). This result correlated well with the superoxide anion accumulation level. The relative superoxide anion levels were *Atccs* > *Atcsd1* > WT (Fig. 15E), indicating that the level of total SOD activity among the three strains was WT > *Atcsd1* > *Atccs*.

When grown on 1/2 MS plates, the seed germination rates of the *Atccs* and *Atcsd1* mutants

were similar to WT (Fig. 15F, control), indicating that the CCS-independent activities in *Atccs* are sufficient for normal growth. With 0.008 or 0.04 μM MV treatments, the seed germination rate of *Atccs* was significantly lower than that of the WT, but was higher than that of *Atcsd1* (Fig. 15F). Similar results were obtained with a 100 μM BH treatment. Hence, although the total CSD activity in *Atccs* was found to be lower than that in *Atcsd1*, the phenotype of *Atccs* (resulting from the CCS-independent CSD activity) is less pronounced than that of *Atcsd1* (resulting from total CSD2 and CSD3 activities).

Root Length of *Atccs* and *Atcsd1* under Oxidative Stress Treatments and Different Glutathione Concentrations

Root length was also measured to compare the phenotype of WT, *Atccs* and *Atcsd1* on treatments with MV and BSO. When *Atccs* was grown on 1/2 MS without paraquat treatment, the root length did not differ from that of the WT (Fig. 16A, 0 μM paraquat), which indicates that the residual CSD activities in *Atccs* were sufficient for plant growth under normal conditions. This finding might also explain why we could not find an obvious phenotype in *Atccs*. However, the root length of WT and *Atccs* was significantly longer than that of *Atcsd1*. Under 0.008, 0.04 and 0.2 μM paraquat treatment, the root length of *Atccs* was shorter than that of the WT but was still longer than that of *Atcsd1* (Fig. 16A). Therefore, although the CSD activities in *Atccs* were lower than that in

Atcsd1, the antioxidant ability resulting from these residual CSD activities in *Atccs* was better than that in *Atcsd1*, which has CSD2 and CSD3 activities. These findings suggest that SOD activities in chloroplasts and peroxisomes cannot efficiently complement the function of the cytosolic SOD. The level of SOD activity should not be the only critical point for the resulting antioxidant ability *in vivo*; whom and where the activities originated were also considerable. We concluded from Fig. 16A that although the 3 CSD activities were diminished in *Atccs*, the residual CCS-independent activities could provide significant protection to cells against oxidative stress. As well, even though the antioxidant ability in *Atccs* was weaker than that in the WT, it was sufficient for normal growth.

However, could the better antioxidant ability of *Atccs* (compared to *Atcsd1*; Fig. 16A) be weakened by glutathione depletion? To answer this, BSO was used to block glutathione biosynthesis in cells; 0.4 mM BSO effectively decreased the internal total and reduced glutathione amount to 16% and 60% (Fig. 16C and 16D), respectively. It has been reported that BSO induces root cell elongation and results in longer root length (Sánchez-Fernández et al., 1997). This can be observed in our treatments that root length became longer when BSO was treated (Fig. 16, comparing B to A), which indicates that the treatments were successful. Notably, with BSO treatment, the root lengths of *Atccs* and *Atcsd1* became similar and were both shorter than that of the WT (Fig. 16B, 0.008 to 0.2 μM paraquat). The root of *Atccs* was originally longer than that of *Atcsd1* with a normal cellular glutathione level (Fig. 16A) but became similar to *Atcsd1* with

decreased glutathione level (Fig. 16B). These findings demonstrate that the better antioxidant ability in *Atccs* conferred by CCS-independent CSD activities were diminished with decreased glutathione concentration, which supported again that internal glutathione was required for CCS-independent activation.

CSD1 Variants Show Differing Activity Levels in Yeast

Previous studies by Carroll et al. (2004) have demonstrated the importance of residues 142 and 144 in the human hSOD1 protein for CCS-independent activation, and showed that substitution of these amino acids with proline prevents activation by this pathway. By aligning CuZnSOD gene sequences in *A. thaliana*, *H. sapiens*, *S. cerevisiae* and *C. elegans* (Figure 17A), the corresponding residues in *Arabidopsis* CSD were found to be 141G/143V in CSD1, 143G/145L in CSD2 and 147S/149V in CSD3. We generated a series of CSD1 mutants: G141A/V143A (denoted CSD1-AA, nematode form), G141S/V143L (CSD1-SL, human form) and G141P/V143P (CSD1-PP, yeast form) to determine the effects of these residues on the CCS-independent activation of CSD1. Each of these variants was expressed individually in yeast *sod1*Δ and *ccs*Δ strains.

The activities of WT CSD1 (CSD1-GV) and CSD1-SL were detectable in both *sod1*Δ and *ccs*Δ, while the activity of CSD1-AA was only measurable in *sod1*Δ (Fig. 17B, lanes 1 to 6). Under lysine-depleted conditions, CSD1-GV and CSD1-SL can restore the lysine-auxotrophic phenotype

of *sod1*Δ and *ccs*Δ (Fig. 17C and 17D). Upon CSD1-AA expression, the viability of *sod1*Δ was restored but that of *ccs*Δ was only partially rescued. Although the activity of CSD1-PP was undetectable in both *sod1*Δ and *ccs*Δ as determined using an in-gel SOD activity assay (Fig. 17B, lanes 7 and 8), the activity of this mutant was discernable using the lysine biosynthesis assay in *sod1*Δ but not in *ccs*Δ (Fig. 17C and 17D). In summary, the *Arabidopsis* form CSD1-GV, the human form CSD1-SL and the nematode form CSD1-AA can be activated by the CCS-independent pathway, but the yeast form CSD1-PP does not undergo CCS-independent activation.

DISCUSSION

Different Activation Preferences of CSD1 and CSD2 Are Due to an Inhibitory Effect of CCS-Independent Activation in Chloroplasts

As characterized in both yeast and *Arabidopsis* protoplasts, it is clear that CSD1 can be activated by both pathways (Figs. 3 and 5D). In contrast, CSD2 could not be activated by CCS-independent pathway in yeast or *Arabidopsis* (Figs. 3 and 5B). Thus, ySOD1 and CSD2 might be activated by a similar mechanism. However, further investigation revealed significant differences between the 2 orthologs. The C-terminal amino acid residues 142P/144P of ySOD1 prevented its activation by the alternative pathway (Carroll et al., 2004), and this effect is mediated primarily by 144P (Leitch et al., 2009a); when 144P is mutated to 144L, this ySOD1 variant showed clear activity in the absence of CCS. For CSD2, the amino acid residues corresponding to 142P/144P of ySOD1 are 143G/145L (Fig. 17A), which are typical for a CSD protein capable of being activated by the CCS-independent pathway (Carroll et al., 2004; Leitch et al., 2009a). The CSD2 protein can be activated by this pathway because the ΔTP-CSD2 (cytoplasm-localized CSD2) was active in *Atccs* (Fig. 5B). Thus, the lack of CCS-independent activity of CSD2 may not result from the protein structure but rather the presence of factor(s) in the chloroplast that inhibit the CCS-independent activation pathway. This hypothesis is supported by the results obtained with the TP_{CSD2}-CSD1 (chloroplast-directed CSD1), which also lost CCS-independent activity (Fig. 5D).

The inhibitory effect on CCS-independent CSD activity in chloroplasts may be due to the absence of chloroplastic factor(s) that are required for CCS-independent activation or to the presence of inhibitory factor(s) in the chloroplast, a novel phenomenon that has not been reported so far for any other species.

The Inhibition of CCS-Independent Activation in Chloroplasts Could Ensure a Proper Operation of the Photosynthesis System

In contemplating the reason for the inhibition of the CCS-independent pathway in chloroplasts, oxygen is one factor worthy of consideration. In CCS-dependent activation, oxygen is required during the disulfide formation between the interacting CCS and CSD proteins (Brown et al., 2004; Furukawa et al., 2004), such that activation cannot occur under hypoxic conditions. Thus, activation by CCS in the chloroplast implies a constant supply of oxygen, which is produced from electron transport chain of the photosynthetic machinery. Such a mechanism can ensure that CSD activation follows the presence of reactive species and oxidants which are produced from a properly functioning photosynthesis. In contrast, CCS-independent activation of CSD does not require oxygen (Leitch et al., 2009a). An additional factor might be related to the fact numerous photosynthetic enzymes require copper as their cofactor (Shcolnick and Keren, 2006). When photosynthetic enzymes are saturated with their copper cofactors, abundant oxygen will be

produced from photosynthesis reactions, which might constitute a signal for CCS to activate CSD. An antioxidant system regulated by oxygen could guarantee that distribution of copper to photosynthetic enzymes takes priority in chloroplasts.

CSD3 Might be Activated Primarily by the CCS-Independent Pathway

Although the CSD3 activity was undetectable by the in-gel SOD activity assay in yeast, it could complement the phenotypes of both yeast *sod1*Δ and *ccs*Δ (Fig. 3), which indicates the presence of a physiologically significant level of CSD activity. In these experiments, the activity in *ccs*Δ could have occurred only through the CCS-independent pathway. However, *sod1*Δ contains factors that can facilitate both CCS-dependent and -independent activation, so phenotype recovery by CSD3 in this system may have occurred by either or both pathways. Thus, these results demonstrate only that CCS-independent activation of CSD3 has occurred, not the level of CSD3 activity that can be conferred by CCS.

To further characterize the activation of CSD3 in a homologous plant system, we did not observe activation with overexpression of the full-length CSD3 in *Arabidopsis* protoplasts. Considering the possible effects of localization similar to CSD2, we deleted its peroxisomal-targeting sequence but still found no activity even with *AtCCS* co-expression (Fig. 6). Kliebenstein et al. (1998) demonstrated similar immunoblotting signals with the same amount (12

ng) of recombinant CSD1, CSD2 and CSD3 protein when probed with α-CSD1, α-CSD2 and α-CSD3 antibodies, respectively. Thus, the amount of overexpressed CSD3 protein in protoplasts should be similar to that of overexpressed CSD1 and CSD2 seen in Fig. 5. Hence, our failure to detect CSD3 activity suggests that its level of activation by CCS is much lower than that of CSD1 and CSD2. In addition, the level of CSD3 activation associated with both pathways (expression in *Atccs* with *AtCCS* co-expression or in wild-type protoplasts) seems not to be significantly higher than the levels associated with the CCS-independent pathway only (expression in *Atccs*). Therefore, CSD3 may be activated primarily by the CCS-independent pathway. Notably, the activation of nematode wSod-1 in the presence of CCS did not result in a higher activity than that by the CCS-independent pathway (Jensen and Culotta, 2005). In this respect, CSD3 seems to be similar to the nematode wSod-1.

Different Preferences for CCS-Dependent and -Independent Activation Might Benefit Life in Its Habitat

To date, studies of CSDs in yeast, nematode, mice and human have shown different preferences for CCS-dependent and -independent activation (Carroll et al., 2004; Jensen and Culotta, 2005; Leitch et al., 2009b). However, our research find a very interesting issue that in *Arabidopsis* that different types of CSDs are present in a single cell (Fig. 18): cytoplasmic CSD1, like human

form, is activated mainly depending on CCS and partially by the CCS-independent pathway; chloroplastic CSD2, like yeast form, activation depends completely on CCS, with inhibition of the alternative pathway in chloroplasts; and peroxisomal CSD3, like nematode form, is activated mainly by the CCS-independent pathway (see previous discussion).

Among the species that have been studied thus far, their habitats are highly varied, so the different preferences for CCS-dependent and -independent activation might imply that the two pathways have advantages in different types of environments. Why different organisms have evolved different preferences for CCS-dependent and -independent activation is unclear but may reflect unique lifestyle requirements for Cu and O_2 (Culotta et al., 2006), which is consistent with our suggestion for the inhibition of CCS activation in chloroplasts. The functions of CCS might be limiting under certain conditions, and the existence of an alternative, CCS-independent pathway might be helpful for survival. Because plants cannot move to avoid environmental stresses, the complex activation mechanisms for plant CSDs might be a solution to cope with such varied and stressful surroundings.

CCS-Independent CSD Activities Are Physiologically Functional and Sufficient to Support Growth of Plant Cells

Upon investigating the physiological effects of the residual CCS-independent activities, we

obtained an unexpected result regarding the higher levels of superoxide anion, seed germination rate and root length of *Atccs* than *Atcsd1*. In trying to understand these results, it should be noted that in *Atcsd1*, CSD1 activity is completely lost, whereas residual CSD1 activity is present in *Atccs*. Since phospholipid membranes are impermeable to O_2^- (Takahashi and Asada, 1983), protection of different organelles can be achieved by variable distributions of SOD in different cellular compartments. In other words, the SOD activities in one compartment cannot complement functional deficiencies in these activities in another. Also, the lower germination rate and the shorter root length of *Atcsd1* were very possibly due to the complete absence of CSD1 activity. In addition, current studies on SODs indicate that the level of SOD activity required for normal growth is much less than the actual activity level measured (Cohu et al., 2009). This can also be observed in yeast. For instance, lysine biosynthesis is recovered by activity that was undetectable by the in-gel assay (Fig. 3), indicating that a small fraction of CuZnSOD activity is enough to protect the enzymes from damage by superoxide anions. In fact, *Atccs* showed no obvious phenotype under normal and stress conditions as compared with WT (Cohu et al., 2009). This demonstrates that loss of the bulk CSD activity did not seriously compromise plant viability. Our observations thus indicate that CCS-independent CSD activities are physiologically functional and sufficient to support the growth of plant cells. One possible reason for the high expression of CSD proteins in WT plants was suggested previously to be their role in copper buffering (Cohu et al., 2009).

CSD1 variants activated by CCS-independent way show different activation efficiency

When mutation forms of CSD1 were expressed in yeast *sod1*Δ line, their activity levels correlated with protein levels (Fig. 17B, lane 1, 3, 5), which indicate that efficiencies of CCS activation of these CSD variants are the same, or differences in such efficiencies were not significant because activation by CCS was too efficient to activate all CuZnSOD protein molecules in these mutant yeasts. However, when they expressed in *ccs*Δ line, activity levels of GV, AA and SL were quite different whereas their protein levels were similar (Fig. 17B, lanes 2, 4, 6). Different activity presented by a similar protein level indicates that partial CSD protein molecules are not activated in the variant with weak activity, and in CCS-independent pathway, the activation efficiency of each variant is different, leading to an observable differences in SOD activity levels..

In addition, levels of activity when one variant is activated by two different mechanisms are not correlated. The form with higher activity by CCS activation was not higher in the alternative pathway, such as GV and AA form of CSD1 for example (Fig. 17B, lanes 1, 2, 3, 4). Thus, activation by CCS or CCS-independently should use totally different mechanisms and even different motifs of CSD protein for the activation Moreover, expression of all variants through the same promoter (yeast PGK promoter) produces very different CSD1 protein levels, indicating residues 142/144 could alter CSD1 protein stability. Taken together, we suggest that only the

functional CuZnSOD was stable when activated via CCS. In the presence of CCS, even though the protein stabilities of variants are different, their activity levels were well-related to their protein levels in *sod1*Δ line. CCS not only activates CuZnSOD functionally but also involved in SOD protein degradation; only the functional protein can survive. On the contrary, in the absence of CCS, CuZnSOD proteins without function can still exist stably in cells, since SOD activity was relatively weak and protein was accumulated in *ccs*Δ line. Therefore, we suggest that the major goal of CCS-independent activation is not to regulate the SOD activity; there should be other role for it, such as Cu buffering.

GSH Is Involved in CCS-Independent Activation Pathway with the Involvement of an Essential Factor Remain to be Discovered

Previous studies of yeast, human, and nematode have shown GSH to be involved in the alternative activation pathway (Carroll et al., 2004; Jensen and Culotta, 2005). Evidence of this involvement includes analyses of a yeast knockout line for GSH biosynthesis, with the major CCS-independent activity abolished. Moreover, when glutaredoxin was knocked out in this system, which resulted in an inability to convert GSSG to GSH, CCS-independent activity was also affected. In our present study, we tested this hypothesis in *Arabidopsis* by overexpressing a glutaredoxin in *Atccs* protoplasts to reduce internal GSH concentrations via enzymatic reactions. However, *ROXY1* expression resulted in a greatly reduced amount of CSD1 protein in addition to reduced activity (Fig.

6B). Because ROXY1 co-localizes with CSD1, it can readily reduce its disulfide bond, which would lead to degradation of disulfide-reduced CSD1 (Borchelt et al., 1994; Wang et al., 2003; Carroll et al., 2006; Rouhier, 2010). In contrast, when we overexpressed *GRXcp*, the GSH concentration decreased, along with CSD1 activity, without a corresponding change in the level of CSD1 protein (Fig. 6B). Although GRXcp can reduce disulfide bonds, it localizes to chloroplasts and cannot interact with CSD1 (Cheng et al., 2006). The effect of GRXcp on CSD1 can therefore be due to only the decrease in GSH concentration. Our result also confirmed the involvement of GSH in this pathway.

However, the results of our *in vitro* experiments show that GSH does not activate CSD1 unless it is added together with cellular extract (Fig. 14). Therefore, GSH may be involved in the CCS-independent pathway in *Arabidopsis*, but cooperation with an additional factor is also required. A deficiency in this unknown factor might explain the limited enhancement in activity with GSH treatments and the lack of association of changes in GSH concentration and CCS-independent activity.

Models of How the Unknown Factor Involves In the CCS-Independent Pathway

Here, we propose two models for CSD activation in absence of CCS (Fig. 19). In the first model, the Cu cofactor is transferred from Cu-GSH complexes to CSD, but interaction between the

Cu-GSH and CSD proteins requires the assistance of an unidentified factor (model A). The role of the unidentified factor is a scaffold protein, which provides a platform for the CSD protein and Cu-GSH to interact. In the second model, Cu is first transferred from Cu-GSH to the unidentified factor and then transferred to a CSD protein (model B). Here, the role of the unidentified factor could be as a Cu carrier, which itself can bind Cu and interact with CSD proteins. Nevertheless, the interaction between CSD and the unidentified factor is essential in either model. Of note, the importance of proline 144 on the carboxyl terminus of hSOD1 has been noted as a potential Cu-GSH docking site of CSD protein (Carroll et al., 2004), which implies the approach of Cu-GSH to the CSD protein (model A), for a more convincing model.

C-Terminal of CSD Protein May Determines Its Activation by CCS or the Unknown Factor

An important difference between CCS-dependent and -independent pathways concerns the status of the CSD disulfide bond (Leitch et al., 2009b). CCS can activate only disulfide-reduced CSD proteins, because the interaction between CCS and CSD involves formation of an intermolecular disulfide bond (Fig. 20A; Culotta et al., 2006). Thus, intramolecular disulfide-oxidized CSD would preclude the interaction (Fig. 20B). In contrast, both disulfide-reduced and -oxidized CSD can be activated by the CCS-independent pathway (Leitch et al., 2009b). This observation led us to suggest that the interaction of CSD and the unidentified

factor differs from that of CSD and CCS, which does not require the formation of the intermolecular disulfide bond (Fig. 20D), so the disulfide-oxidized CSD can still interact with the unidentified factor (Fig. 20E).

As mentioned previously, the presence of proline at position 144 of ySOD1 prevents activation by the CCS-independent pathway (Fig. 17; Carroll et al., 2004; Jensen and Culotta, 2005). The most recent model indicates that this proline results in a conformational restriction that prevents disulfide bond formation within CSD in the absence of CCS (Leitch et al., 2009b). This restriction on disulfide bond formation can be overcome by the action of CCS but not the CCS-independent mechanism (Fig. 20, C and F, respectively). Here, we suggest another reason for an essential unidentified factor in CCS-independent pathway interacting with the disulfide-oxidized CSD. In this model, the molecular conformation adopted by CSD containing proline 144 may prevent interaction of the unidentified factor with the CSD protein. This situation would explain why proline 144 blocked only CCS-independent activity but not that conferred by CCS. Further investigation is required to characterize the unidentified factor and elucidate the complete mechanism.

PERSPECTIVES

In this thesis, we address an important finding of the CCS-independent activation of three CSDs in the *Arabidopsis*. Thus, our future research will be to reveal the detail CCS-independent activation mechanism, and its effect to plants. The following are the major aspects: (1) Identify the unknown factor which involved in the CCS-independent pathway; (2) Test the effects of the oxygen on the CCS-independent activation; (3) Investigate the disulfide status of the three CSDs in two activation pathways; (4) Identify the phenotype of the *SOD*-knockout lines during different oxidative stress. Detail descriptions are as follows:

Search of the unknown factor which involved in the CCS-independent pathway

In an attempt to understand the CCS-independent activation mechanism, we will identify the unknown factor(s) which cooperates with GSH to activate CSD. In this effort, the *Atccs*-cellular extract will be fractionated by chromatography of ion exchange, gel filtration, and reverse-phase HPLC. Apo-CSD1 will be treated with the fractions to see activity recovery *in vitro*, the most effective fractions will be sent for LC-MS/MS analysis to identify the potentials factors.

The factors identified by LC-MS/MS will then be tested in various methods to confirm their relations to CCS-independent activation. Experiments can be performed with the recombinant protein, and the protoplast overexpression system to analyze the variation of the CSDs activities.

And, we can use yeast-two hybrid system and BiFC to observe its interaction with CSDs. We also can observe the phenotype of the *Arabidopsis* knockout/overexpression mutants of each gene, or analysis the domain function of the factors as further investigations.

Effect of the molecular oxygen in the CCS-independent activation

It has proved that CCS activation of SOD1 requires molecular oxygen (Brown et al., 2004). However, there is no similar oxygen dependence with CCS-independent activation in human SOD1 (Culotta et al., 2009). Inhibition of CCS-independent activation of *Arabidopsis* chloroplastic CSD2 might also be a hint for a key role of oxygen in determining the dependence of CSD activation (see our discussion). Hence, we are curious about the relation between oxygen conditions to the CCS-independent activation in *Arabidopsis*. Thus, we will overexpress the CSDs in WT and *Atccs* protoplasts, and measure the changes of SOD activity under hypoxic and anoxic treatments.

Comparing the ratio of the CSD disulfide status between two activation pathways

Disulfide of SOD proteins is firstly shown to be oxidized by Cu-CCS during activation processes (Furukawa et al., 2004). However, the disulfide of *C. elegans* CuZnSOD is retained in the oxidized state regardless of copper or CCS conditions, and the disulfide of human SOD1 is also ~50% oxidized in the absence of CCS and copper (Culotta et al., 2009). It is hypothesized that CCS

can only activate disulfide-reduced SOD, and CCS-independent activation can activate SOD with either reduced or oxidized disulfide bond, which make the SOD disulfide bond status be a good indicator for researches in the two activation pathway. Since the three *Arabidopsis* CSDs show different preference to the CCS-dependent and -independent activation, their ratio of the disulfide status might be very different. For example, the disulfide bond status of CSD2 (which is suggested to fully depend on CCS) should show more reduced form than CSD1, and CSD3 (which is suggested to be CCS-independent) should show more oxidized form than CSD1. In this effort, we can use AMS (4-acetamido-4'-maleimidylstilbene-2,2'-disulfonic acid) treatment to compare the disulfide status between CSDs in WT and *Atccs*, including three *Arabidopsis* CSD proteins (CSD1, CSD2, CSD3), CSD proteins delivered to different compartments (TP2-CSD1, ΔTP-CSD2, CSD3-ΔAKL), and variants of CSD1 (CSD1-AA, CSD1-SL, and CSD1-PP). We can also observe the variation of the CSDs disulfide status after different concentration of GSH, or copper treatments. These results should be supporting evidences of our CSDs activation preference model, and also provide information for researches in the CCS-independent activation mechanism.

Phenotype observations of the SOD knockout lines during different oxidative stress

Superoxide dismutases are conserved in evolution, which suggests important functions of these proteins. However, it is surprising that there are no obvious phenotypes in *Atcsd1* and *Atccs*

(Fig. 15, 16; Cohu et al., 2009; Chu et al., 2005). It can be explained by the functional complement of the different SODs, or other purposes (such as copper pool) for the highly expression SODs level under normal conditions (our discussion; Cohu et al., 2009). To answer this, we need to collect more information, especially in phenotypes of various SOD-knockout mutants. First, we can compare the phenotypes between different CSD-knockout lines, double-knockout lines under different oxidative stresses. We also can observe the phenotype of the *fsd1*/*Atccs* double-knockout mutant, which loses both the FSD1 and CSD2 activity in chloroplast, to help us understand the role of SOD in the chloroplast. Comparing the *Atcsd1/Atccs* double-knockout mutant (with no CSD1 protein and loses both CSD1 and CSD2 activities, which has CSD2 protein only) with *Atcsd1* (with no CSD1 protein and activity, which has both the CSD2 protein and activity) to show the unknown function of CSD2 protein. Comparing the phenotype of *Atccs*/ΔTP-CCS (has CSD2 proteins but with no CSD2 activity) with *Atcsd2* (with no CSD2 protein and activity) can help us to discriminate the function of the SOD protein itself (but not its activity). Similarly, comparing the *Atccs*/CCS-ΔSKV (which may or may not has CSD3 activity but has the CSD3 protein) with *Atccs* (with normal CSD3 protein and activity) and *Atcsd3* (with no CSD3 protein and activity) may help us to confirm the CSD3 activation preference and its unknown function.

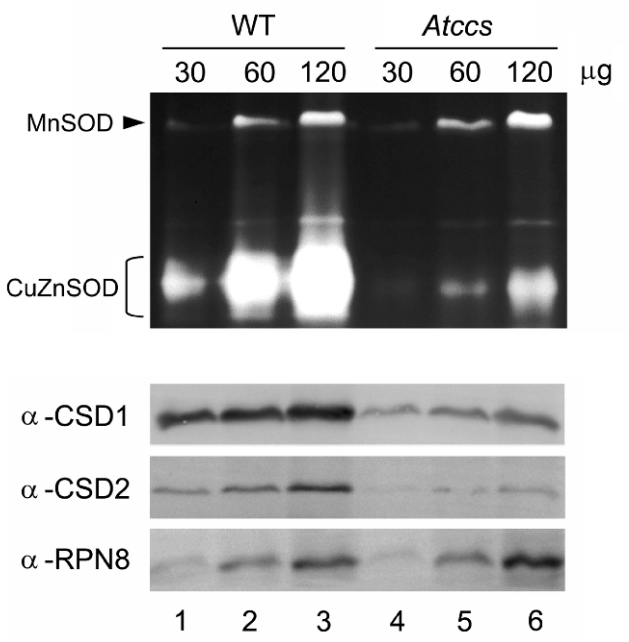

Figure 1. Residual CSD activities in *Arabidopsis AtCCS*-deleted flowers.

Crude protein extracts of 45-d-old *Arabidopsis* wild-type (WT) and *Atccs* flowers were analyzed for SOD activity (top) and CSD1 and CSD2 protein levels (bottom). No CSD3 protein was detected and the data is not presented here. A 26S proteasome regulatory subunit RPN8 was used as a loading control. Thirty (lanes 1 and 4), 60 (lanes 2 and 5) and 120 μg (lanes 3 and 6) of total protein were loaded, as indicated. The percentage of CCS-independent activity represents an average of at least four replicates and was calculated relative to the wild type activity.

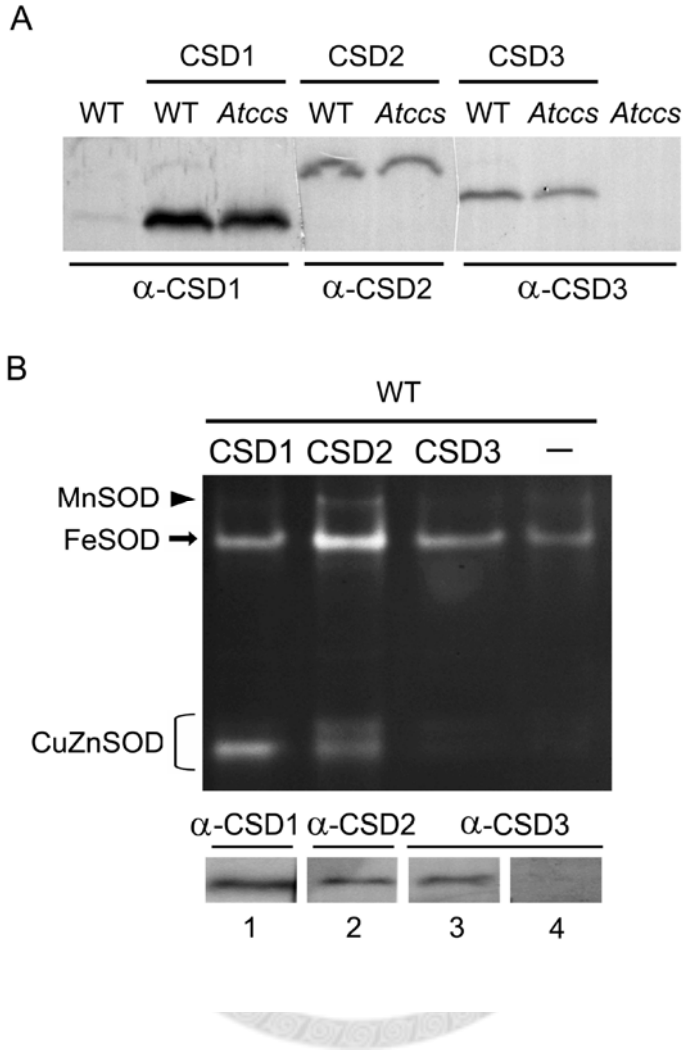

Figure 2. Transient expression of CSD genes in the *Arabidopsis* WT and *Atccs* protoplasts.

(A) Characterization the transiently expressed CSD1 (15 kD), CSD2 (22 kD) and CSD3 (16.9 kD) proteins in the WT and *Atccs* protoplasts by immunoblotting. The input amount protoplasts of *Atccs* (~7.5×10^5 cells) was 3-fold higher than that of the WT (~2.5×10^5 cells). (B) The activity (top panel) and protein amount (bottom panel) of CSD1, CSD2 and CSD3 were analyzed in the WT protoplasts. Lane 4 was the protoplast extracts without transfection as a control.

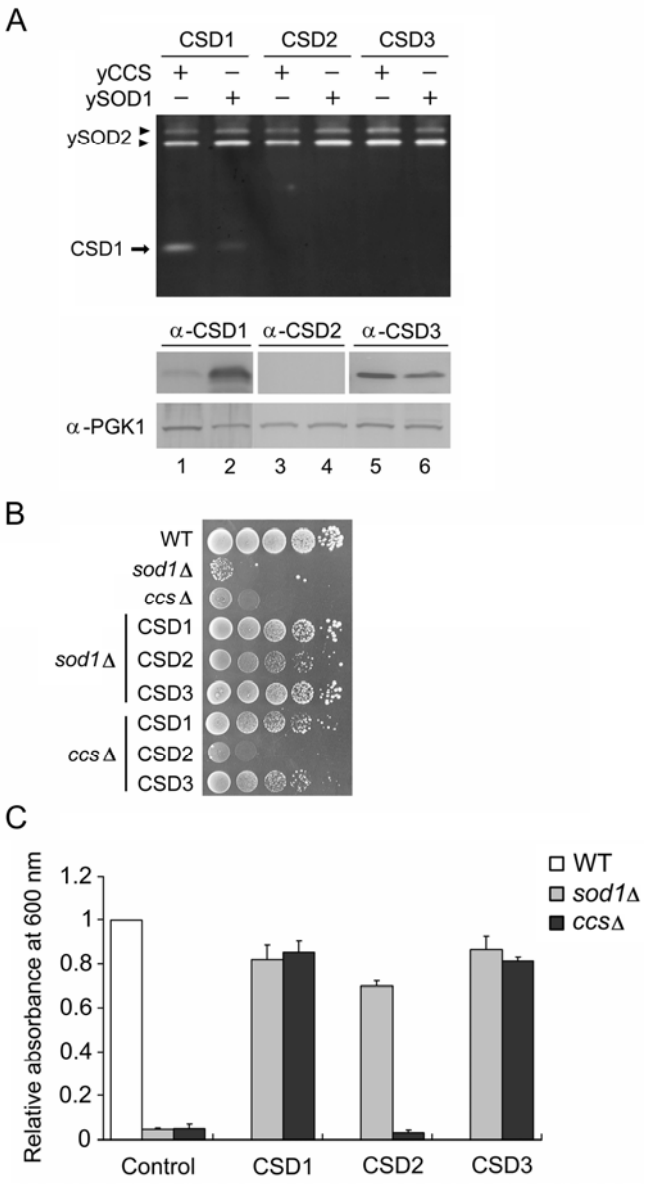

Figure 3. The activities of three CSDs expressed in yeast *sod1*Δ and *ccs*Δ.

(A) Lysates of yeast expressing CSD1, CSD2 and CSD3 were analyzed by the in-gel SOD activity assay (top) and immunoblotting (bottom) with 150 μg and 15 μg of total protein, respectively.

Phosphoglycerate kinase 1 (PGK1) is a loading control for the yeast extract. Strains expressed on *sod1*Δ or *ccs*Δ background were represented as yCCS+/ySOD1− and yCCS−/ySOD1+, respectively. (B) and (C) The viability of yeast deletion strains *sod1*Δ and *ccs*Δ expressing CSD1, CSD2 or CSD3 under lysine lacking conditions. Experimental procedures describing the plate (B) and liquid (C) assays can be found in Materials and Methods. Values of cell density were expressed relative to the WT level. All data were from at least four independent tests (mean ± SD).

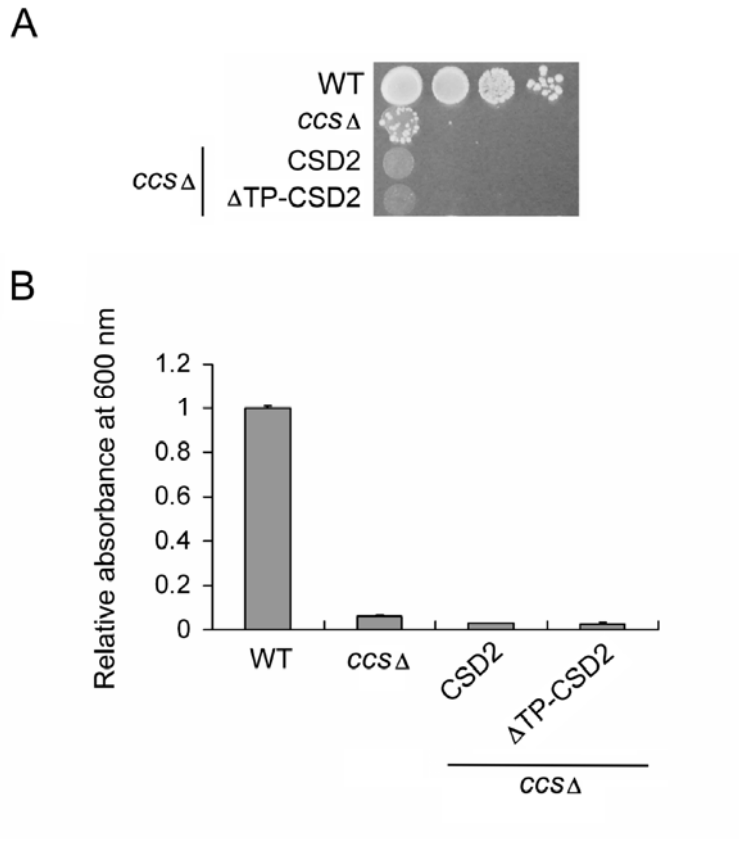

Figure 4. The viability of yeast *ccs*Δ expressing CSD2 with or without transit peptide under lysine lacking condition.

Full-length and chloroplast transit peptide deleted CSD2 (ΔTP-CSD2) were expressed in yeast *ccs*Δ, and then the plate (A) and liquid (B) assays were performed as described in Fig. 3. Yeast WT and *ccs*Δ were used as references.

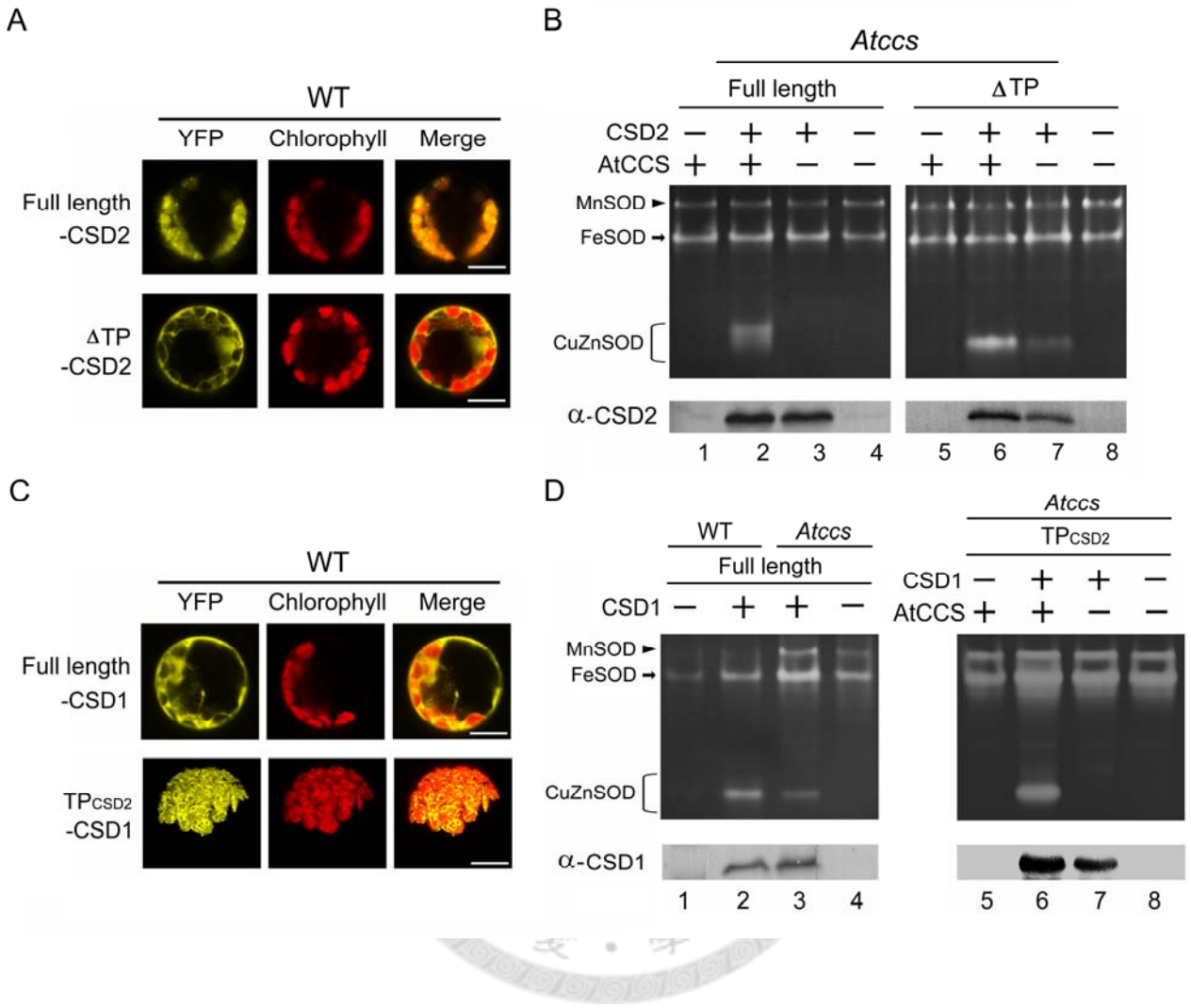

Figure 5. Localization and SOD activity of CSD1 and CSD2 overexpressed in *Atccs* protoplasts.

(A) and (C) YFP fusion proteins of full length- and chloroplast transit peptide deleted- (ΔTP)-CSD2 (A), and YFP fusion proteins of full length-CSD1 and that fused to the chloroplastic transit peptide (TP_{CSD2}-CSD1) of CSD2 (C), were expressed in *Arabidopsis* WT protoplasts for localization analysis. The chloroplasts are visualized as red autofluorescence. Bars, 10 μm.

(B) and (D) Full length- and ΔTP-CSD2 (B), and full length- and TP_{CSD2}-CSD1 (D) were overexpressed with or without AtCCS co-expression in *Atccs* or WT protoplasts, after which CSD activity (top) and protein amount (bottom) were analyzed. The CSD genes used here contained no YFP fusion. Because CSD protein expression was reduced in *Atccs* (Fig. 1, bottom), we loaded threefold more *Atccs* protoplasts (~7.5×10^5 cells) than WT protoplasts (~2.5×10^5 cells), in order to present a similar protein level in the result.

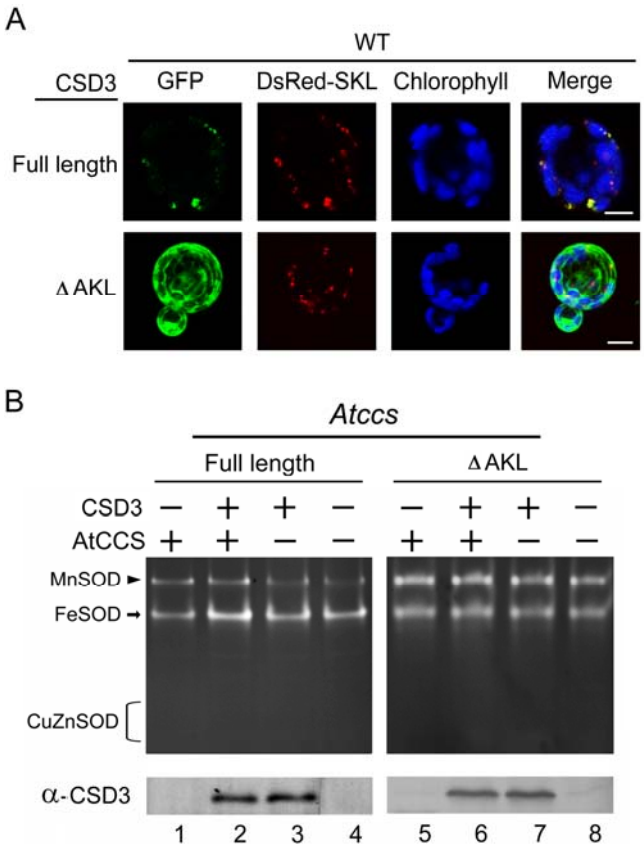

Figure 6. Localization and SOD activity of full length and AKL-deleted CSD3 overexpressed in *Arabidopsis* protoplasts.

(A) GFP fusion proteins of full length and C-terminal AKL deleted (ΔAKL)-CSD3 were expressed in *Arabidopsis* WT protoplasts for localization analysis. DsRed-SKL is a peroxisomal marker. The autofluorescence of chlorophyll is depicted in blue. Bars, 10 μm. (B) Full length- and ΔAKL-CSD3 were overexpressed with or without AtCCS co-expression in *Atccs* or WT protoplasts, after which CSD3 activity (top) and protein amount (bottom) were analyzed. The CSD genes used here

contained no GFP fusion.

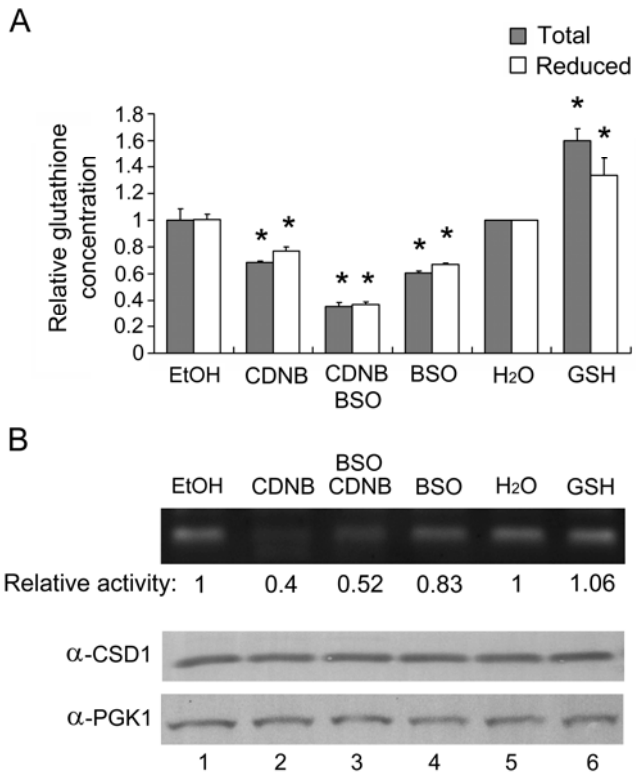

Figure 7. The activity of CSD1 expressed in yeast *ccs*Δ with different glutathione concentrations.

One mM CDNB, 1 mM BSO or 20 mM GSH were used in the treatments as indicated. Equal volumes of 95% ethanol (EtOH) or H_2O were added as mock treatments of CDNB and GSH. (A) Cellular concentrations of total and reduced glutathione in the yeast lysates were analyzed after treatments. Data represent results of three independent experiments (means ± SD). Values are relative to the H_2O control (treatment 5). ∗, $P < 0.05$ (Student's *t* test). (B) CSD1 activity (top) and protein amount (bottom) were analyzed following the treatment using 150 and 15 μg total protein,

respectively. The values below the activity gel are values relative to the mock control. Bands were quantified using ImageQuant software. PGK1 was used as a loading control.

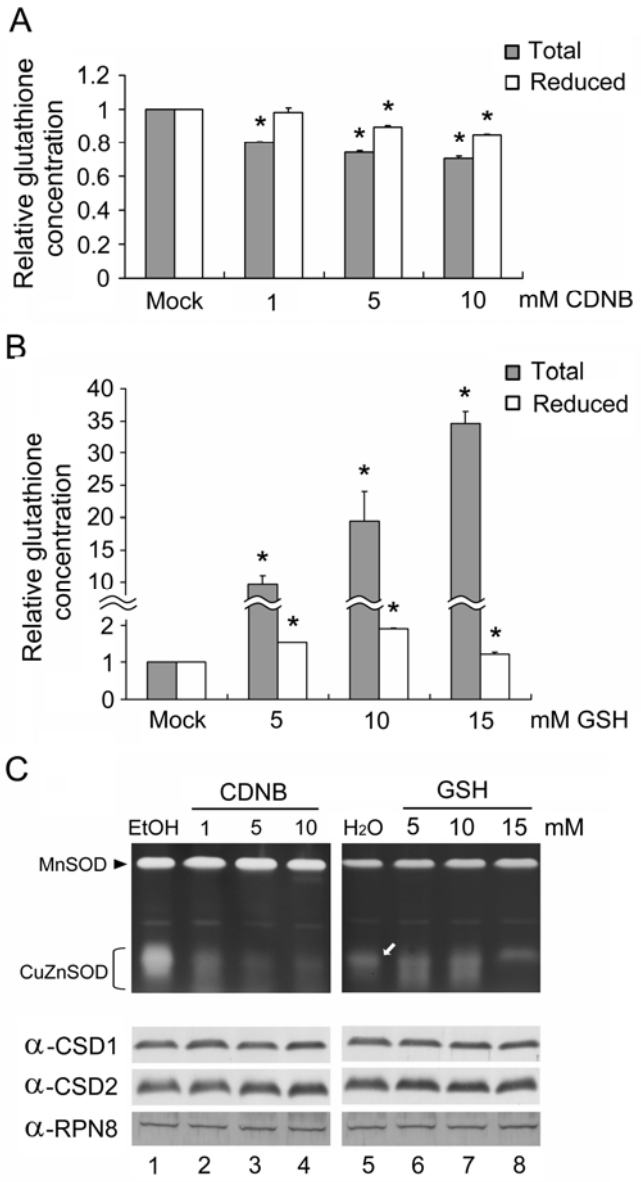

Figure 8. The effect of glutathione level on CCS-independent CSD activity in *Atccs* flowers.

Flowers taken from *Atccs* plants were soaked in CDNB or GSH solutions at the indicated concentrations for 3 or 1 h, respectively. Equal volumes of 95% ethanol (EtOH) or H_2O were added as mock treatments of CDNB and GSH.

(A) and (B) Cellular concentrations of total glutathione (gray bar) and GSH (white bar) in *Atccs* flowers treated with CDNB (A) or GSH (B). The values are relative to those of the mock treatments. Data represent results of three independent experiments (means ± SD). ∗, $P < 0.05$ (Student's *t* test). (C) SOD activity (top) and CSD1 and CSD2 protein amounts (bottom) were analyzed using 150 μg and 30 μg total protein, respectively. RPN8 was used as a loading control. A white arrow in the lower part of the GSH-treatment activity gel indicates the location of the major CSD activity band.

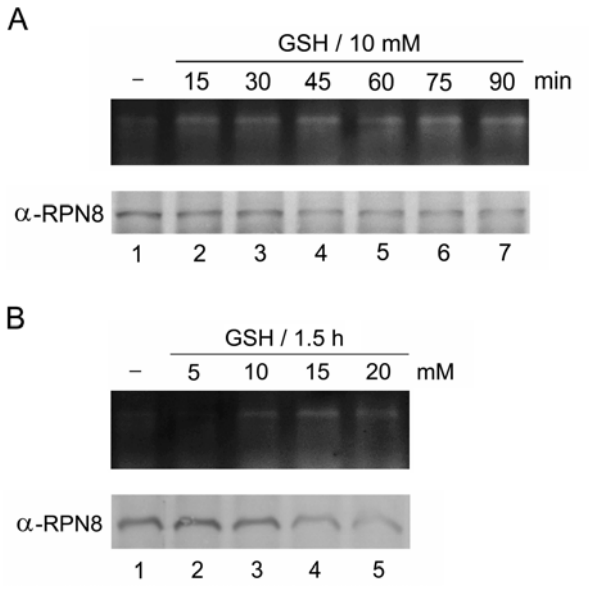

Figure 9. CSD activities in *Atccs* flower protein extract treated with GSH in vitro.

The *Atccs* flower protein extract was treated with 10 mM GSH for different incubation time (A) or with GSH at different concentrations for 1.5 h (B). Lane 1 presents a mock treatment in panels (A) and (B). RPN8, an internal reference protein, exhibited decreased accumulation and/or stability high GSH concentrations.

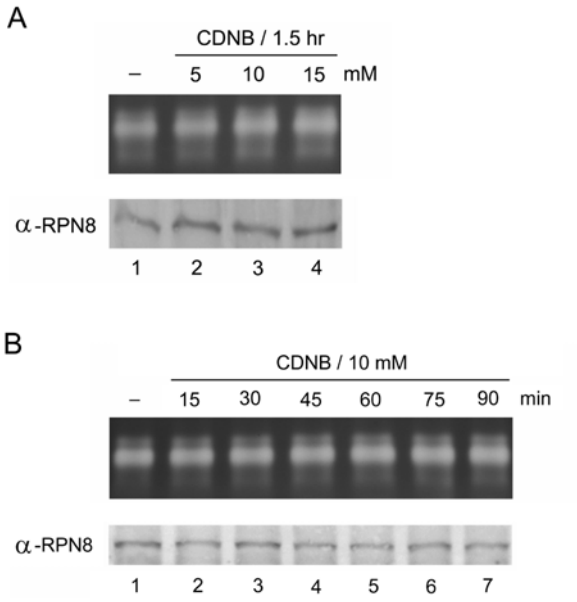

Figure 10. The CuZnSOD activities of WT flower protein extract treated with CDNB *in vitro*. (A) and (B) CDNB was added into the protein extract at different concentrations for 1.5 h incubation (A) or with 10 mM for different incubation time (B). After incubation, CDNB solutions were removed, and the flowers were washed with water 3 times, then the WT flower protein extract was analyzed for CSD activities. Lane 1 in both (A) and (B) was a mock treatment. RPN8 was a loading control.

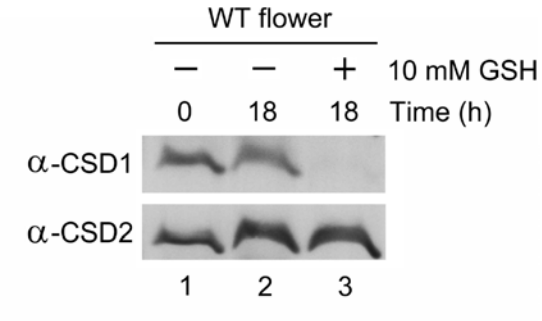

Figure 11. CSD1 and CSD2 protein levels in WT flower protein extract treated with GSH *in vitro*.

The WT flower protein extract was treated without or with 10 mM GSH and incubated at 30°C for 18 h, then protein levels were analyzed by use of α-CSD1 and α-CSD2 antibodies. An aliquot of the same plant extract was stored at −20°C and then used as a control (lane 1).

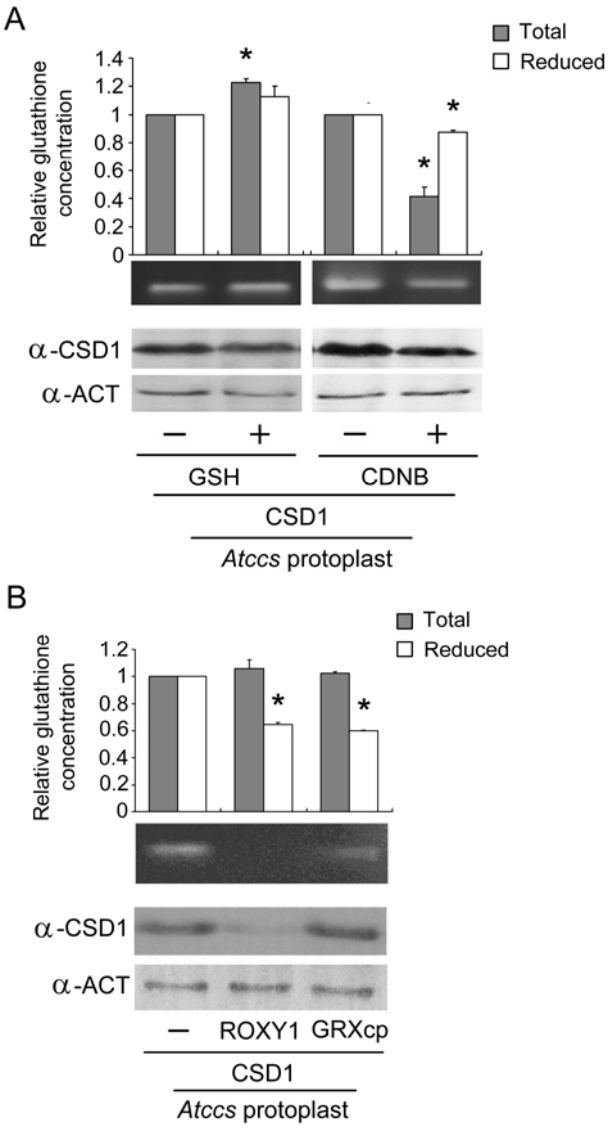

Figure 12. The effect of glutathione concentration on the activity of CSD1 transiently expressed in *Arabidopsis* protoplasts.

(A) *Atccs* protoplasts overexpressing CSD1 were treated with 5 mM GSH or 5 mM CDNB for 2 h as indicated. After incubation, extracts of these protoplasts were analyzed for their cellular

concentrations of total glutathione and GSH, SOD activity, or amount of CSD1 protein. Actin (ACT) was used as an internal control. (B) CSD1 was transiently expressed in *Atccs* protoplasts together with ROXY1 or GRXcp. Extracts of these protoplasts were analyzed for their cellular concentrations of total glutathione and GSH, SOD activity, or amount of CSD1 protein. ACT was used as an internal control. Data represent results of three independent experiments (means ± SD). ∗, $P < 0.05$ (Student's *t* test).

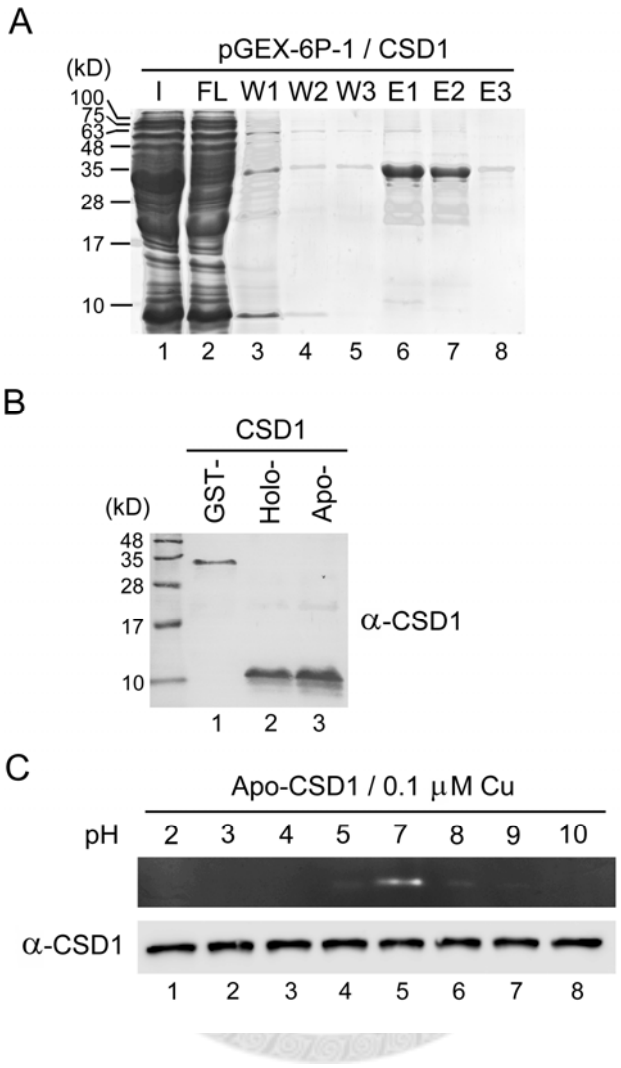

Figure 13. Purification and characterization of recombinant CSD1 proteins.

(A) The *CSD1* gene was cloned into the pGEX-6P-1 vector for fusion with a GST tag. Twenty μL of the samples at each step was subjected to SDS-PAGE and Coomassie Blue staining. I, IPTG induced cellular extract. FL, flow through. W1–W3, wash. E1–E3, eluate. (B) Fifty ng each of purified GST-, and GST digested Holo- and Apo-CSD1 was analyzed by immunoblotting. (C) The

activity of 870 ng Apo-CSD1 incubated with 0.1 μM Cu was analyzed after the indicated treatments. Buffers used for each pH were: 0.2 M Na_2HPO_4 and 0.1 M citrate for pH 2–7, and 0.2 M glycine-NaOH for pH 9–10.

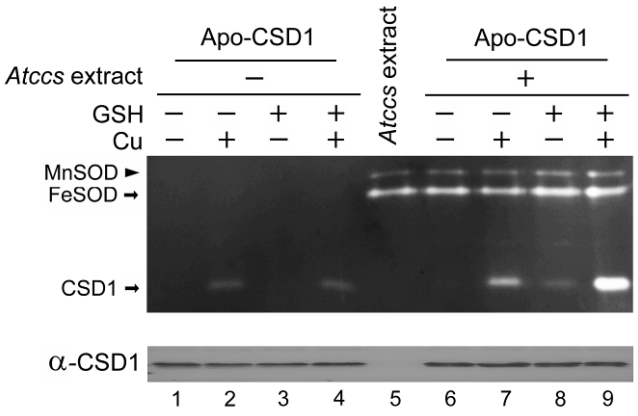

Figure 14. Activation of Apo-CSD1 by Cu, GSH and *Atccs* leaf cellular extract.

The activity of Apo-CSD1 was analyzed by the in-gel SOD activity assay following the indicated treatments (top). Each reaction contained 870 ng Apo-CSD1 protein and 20 μM $ZnSO_2$, except for lane 5, which contained only 15 μg *Atccs* cellular extract and served as a control for extract-containing samples. For GSH, Cu or *Atccs* cellular extract treatments, 1 mM, 0.1 μM and 15 μg of these additions were used, respectively. Both the native-gel and the running buffer contained 0.1 mM EDTA. A replicate with the same treatments on 50 ng Apo-CSD1 was used for analyzing the amount of CSD1 protein by immunoblotting (bottom).

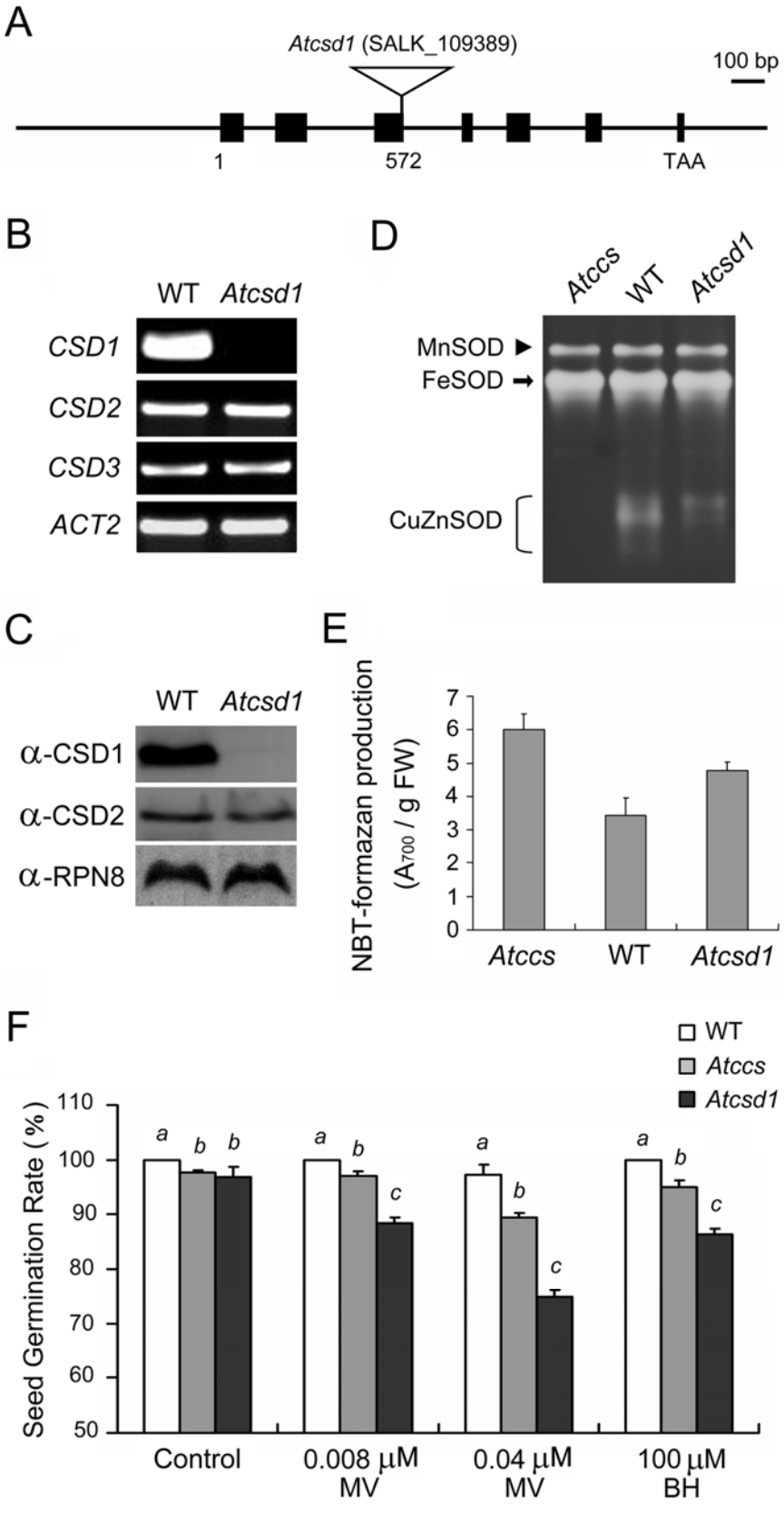
A
Atcsd1 (SALK_109389)
100 bp
1
572
TAA
B
WT
Atcsd1
CSD1
CSD2
CSD3
ACT2
D
Atccs
WT
Atcsd1
MnSOD
FeSOD
CuZnSOD
C
WT
Atcsd1
α-CSD1
α-CSD2
α-RPN8
E
NBT-formazan production
(A700 / g FW)
0
1
2
3
4
5
6
7
Atccs
WT
Atcsd1
F
WT
Atccs
Atcsd1
Seed Germination Rate (%)
110
100
90
80
70
60
50
a
b
b
a
b
c
a
b
c
a
b
c
Control
0.008 μM MV
0.04 μM MV
100 μM BH

Figure 15. Characterization and seed germination rate of the WT, *Atccs* and *Atcsd1*.

(A) T-DNA insertion site of the *CSD1*-knockout plant, *Atcsd1*, can be found at the third exon of the *CSD1* gene (572th nucleotide of the genomic sequence). (B) Gene expression levels of *CSD1*, *CSD2* and *CSD3* in 7-d-old WT and *Atcsd1* seedlings. *Actin2* (*ACT2*) was used as a loading control. (C) CSD1 and CSD2 protein levels in WT and *Atcsd1* seedlings. RPN8 was used as a loading control. (D) SOD activities of the WT, *Atccs* and *Atcsd1*. Thirty μg of the protein extract from 7-d-old seedlings was analyzed. The CuZnSOD activity level is generally lower in seedlings, thereby the residual activity in lane 1 is unable to be detected. (E) Superoxide anion level of the WT, *Atccs* and *Atcsd1* plants was analyzed by measuring the NBT-formazan production level in 7-d-old seedlings. Data represent results from three independent experiments (means ± SD). (F) The seed germination rate of the WT, *Atccs* and *Atcsd1* plants grown on 1/2 MS plates with 100 μM BH, 0.008 or 0.04 μM MV treatments was analyzed. Data represent results from five independent experiments (means ± SD). a, b and c indicate different statistic groups between WT, *Atccs* and *Atcsd1* in each treatment at $P < 0.05$ (Student's *t* test).

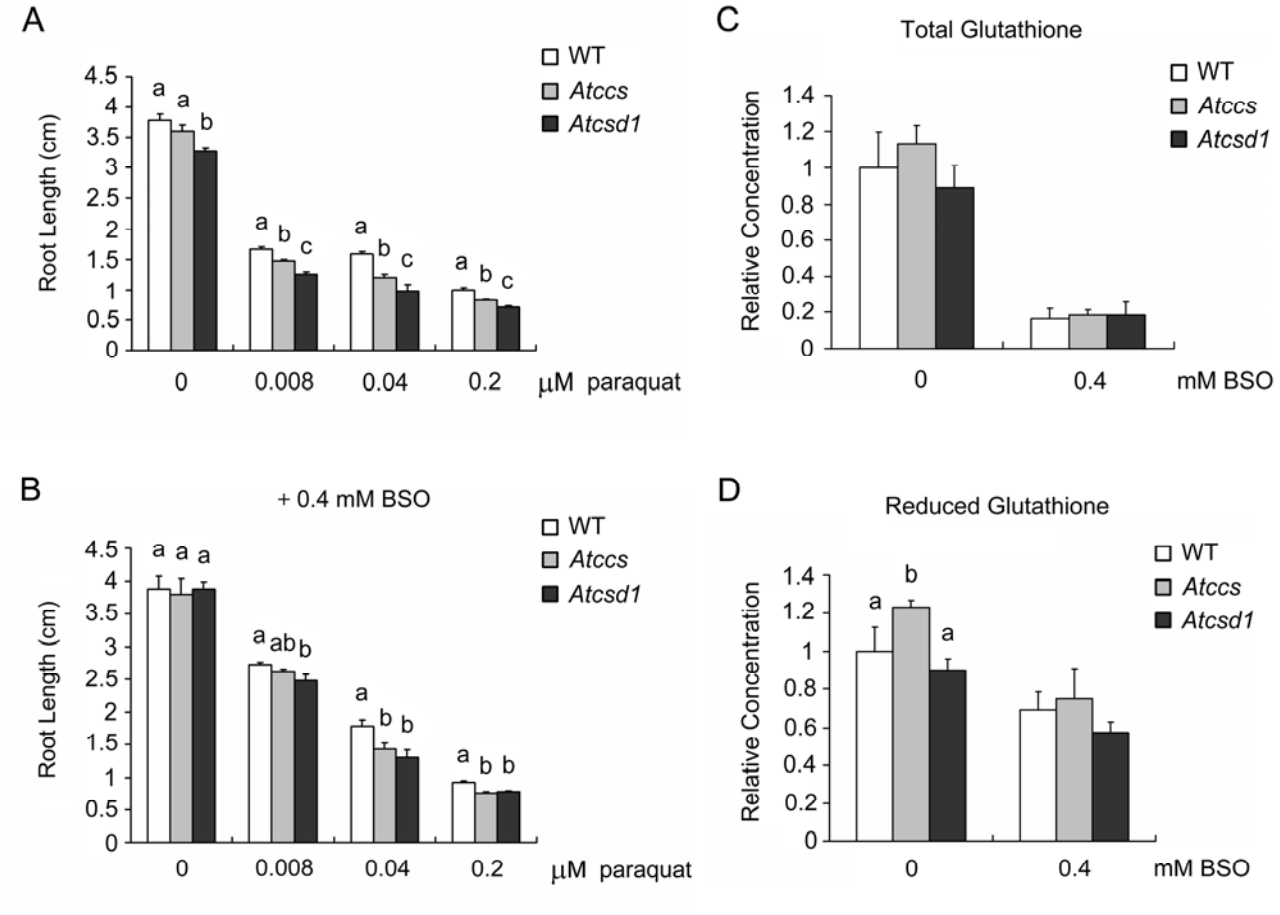

Figure 16. The antioxidant abilities in WT, *Atccs* and *Atcsd1* with paraquat and BSO treatments.

(A) and (B) Root length of WT (white bar), *Atccs* (gray bar) and *Atcsd1* (black bar) grown on 1/2 MS plates with 0, 0.008, 0.04 and 0.2 μM paraquat treatment (A) or additionally with 0.4 mM BSO (B) for 4 d. Different statistic groups with $P < 0.05$ are indicated as *a*, *b* and *c* and was assessed by two-tailed, unequal-variance Student's *t* test. (C) and (D) Total (C) and reduced (D) glutathione

concentration of plants grown on 1/2 MS plates without or with 0.4 mM BSO treatment were measured and presented as values relative to that of WT without treatment. All data was determined in 3 independent experiments from 16 plants per line of each treatment (means ± SD). Under the normal condition, the reduced glutathione concentration in *Atccs* was significantly higher than that of the WT (panel D).

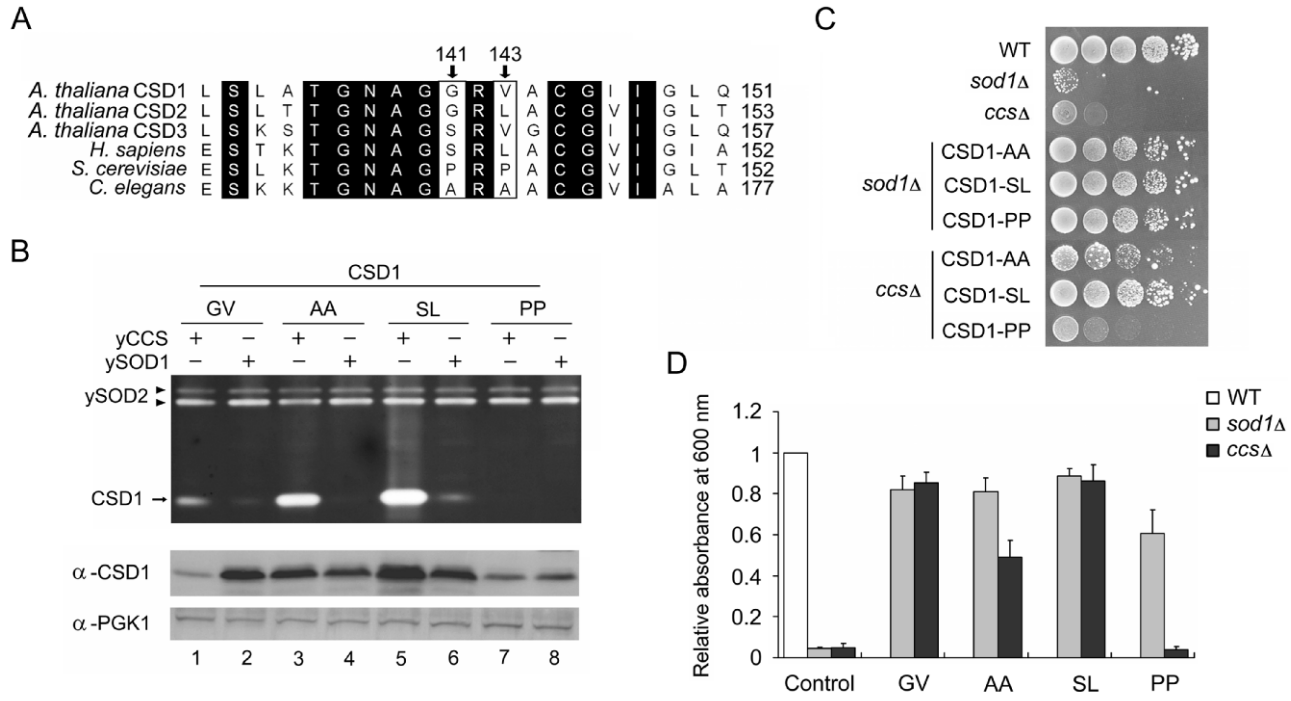

Figure 17. Expression of *Arabidopsis* CSD1 variants in yeast *sod1*Δ and *ccs*Δ.

(A) Amino acid sequence alignment of CuZnSOD genes in *A. thaliana* (CSD1, CSD2 and CSD3), *H. sapiens* (hSOD1), *S. cerevisiae* (ySOD1) and *C. elegans* (wSod-1). Residues corresponding to 141G and 143V of CSD1 are indicated in the open boxes with arrows. Black boxes highlight identical residues. (B) Yeast strains expressing the CSD1 variants in *sod1*Δ and *ccs*Δ were analyzed as described in Fig. 3A for SOD activity (top) and CSD1 protein levels (bottom). (C) and (D) The viability of yeast strains *sod1*Δ and *ccs*Δ expressing the CSD1 variants under lysine lacking conditions. Plate (C) and liquid (D) assays were performed as described in Fig. 3B and 3C. The data were taken from at least four independent tests (mean ± SD).

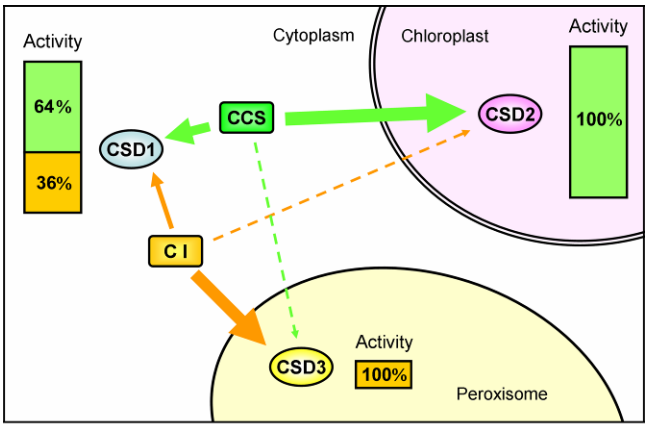

Figure 18. Summary of different activation dependence of the three *Arabidopsis* CSDs.

Assuming that the total activity of each CSD in the WT is 100%, the fraction activated by AtCCS (CCS) is represented in green and that activated through the CCS-independent (CI) pathway is represented in orange. Solid lines stand for the activation which was demonstrated experimentally, and the dashed lines indicate undetectable activation. Based on our results, we propose that cytosolic CSD1 is activated mainly by CCS and partially by a CCS-independent pathway. The level of CCS-independent CSD1 activation was ~36% of that in WT (Fig. 5D, lanes 2 and 3). CSD2 in chloroplasts should be activated completely by CCS (Fig. 5B, lanes 2 and 3), whereas most activity of peroxisomal CSD3 might be conferred by the CCS-independent pathway (see Discussion).

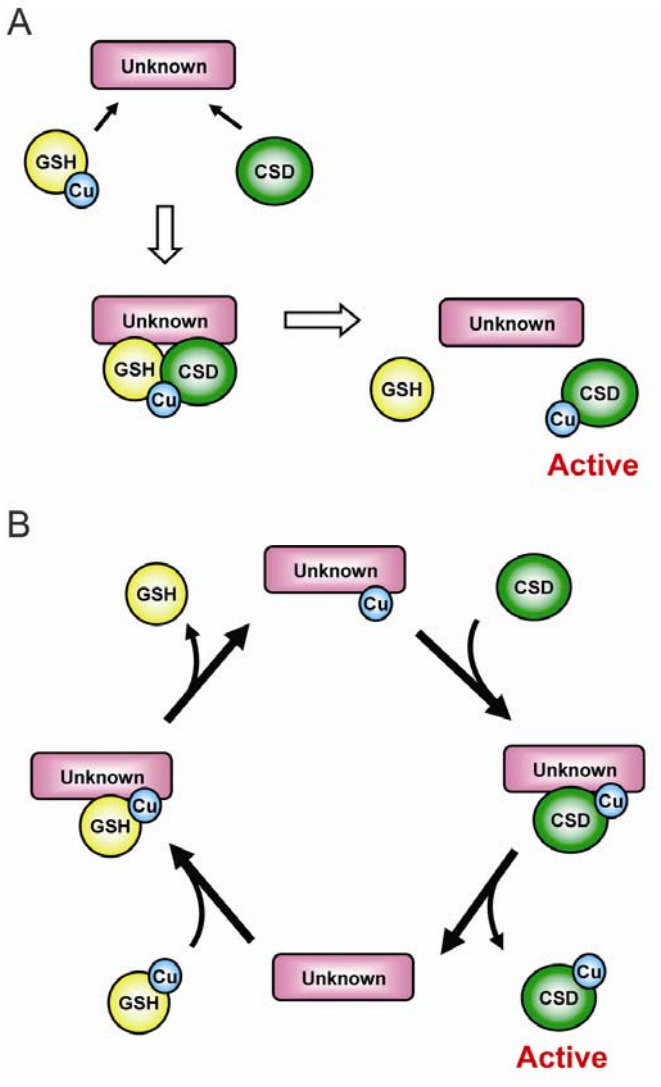

Figure 19. Two possible models for CCS-independent activation of CSD.

(A) The unidentified factor (unknown), which acts like a scaffold protein, first interacts with both GSH and the CSD protein, and the GSH-bound Cu cofactor is then transferred to CSD. (B) The Cu cofactor is first transferred from GSH to the unidentified factor and then transferred to a CSD protein. In this model, the unidentified factor functions as a Cu carrier.

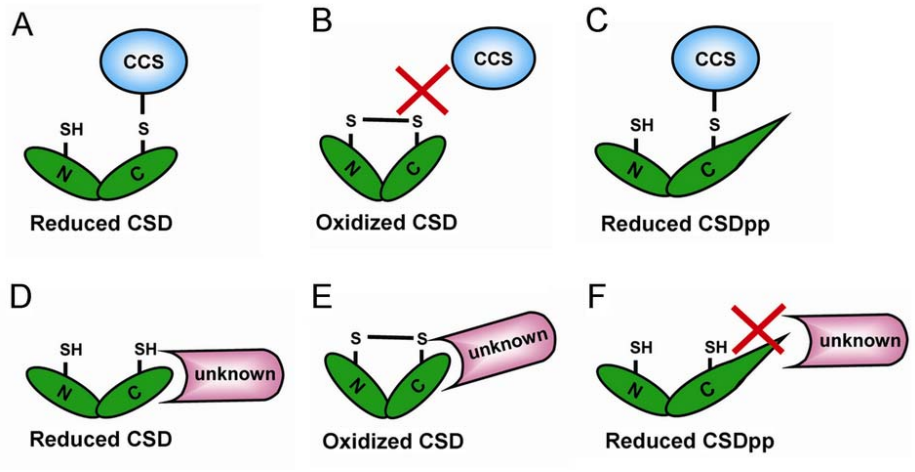

Figure 20. CSD interacts with the CCS versus the unidentified factor.

(A) to (C) The CCS interacts with disulfide-reduced CSD and CSD_{PP} but not disulfide-oxidized CSD. (D) to (F) The unidentified factor (unknown) interacts with disulfide-reduced and -oxidized CCS but not CSD_{PP}

Table 1. Accession numbers of genes described in this article.

Gene	**Genus species**	**Accession number**
AtCCS	*Arabidopsis thaliana*	NP_563910.2
CSD1	*Arabidopsis thaliana*	NP_001077494.1
CSD2	*Arabidopsis thaliana*	NP_565666.1
CSD3	*Arabidopsis thaliana*	NP_197311.1
ROXY1	*Arabidopsis thaliana*	NP_186849.1
GRXcp	*Arabidopsis thaliana*	NP_191050.1
hSOD1	*Homo sapiens*	NP_000445.1
ySOD1	*Saccharomyces cerevisiae*	NP_012638.1
wSod-1	*Caenorhabditis elegans*	NP_001021956.1

Table 2. Primer pairs used in this research.

The mutation sites of CSD1 are underlined.

Construct	**Primer Set**	**Sequence (5′ to 3′)**
CSD1-AA mutation	G141A/V143A-Fw	AACGCAGGCGCCCGTGCTGCTTGCGGC
	G141A/V143A-Rv	GCCGCAAGCAGCACGGGCGCCTGCGTT
CSD1-SL mutation	G141S/V143L-Fw	AACGCAGGCTCCCGTCTTGCTTGCGGC
	G141S/V143L-Rv	GCCGCAAGCAAGACGGGAGCCTGCGTT
CSD1-PP mutation	G141P/V143P-Fw	AACGCAGGCCCCCGTCCTGCTTGCGGC
	G141P/V143P-Rv	GCCGCAAGCAGGACGGGGGCCTGCGTT
Full length CSD2 (and RT-PCR)	CSD2-Fw-NcoI	TCTCCATGGCTGCCACCAACACAATCCT
	CSD2-Rv	TTAGAGCGGCGTCAAGCCAATCA
ΔTP-CSD2	ΔTP-CSD2-Fw-HindIII	CAAAGCTTATGTCCGCGGCGAAGAAGGCT
	CSD2-Rv	TTAGAGCGGCGTCAAGCCAATCA
Full length CSD2-YFP	CSD2-Fw-NcoI	TCTCCATGGCTGCCACCAACACAATCCT
	CSD2ns-Rv-SalI	CAGTCGACCCGAGCGGCGTCAAGCCAATCA
ΔTP-CSD2-YFP	ΔTP-CSD2-Fw-HindIII	CAAAGCTTATGTCCGCGGCGAAGAAGGCT
	CSD2ns-Rv-SalI	CAGTCGACCCGAGCGGCGTCAAGCCAATCA
Full length CSD1 (and RT-PCR)	CSD1-Fw-NcoI	TCTCCATGGCGAAAGGAGTTGCAGTTTT
	CSD1-Rv	TTAGCCCTGGAGACCAATGATGC
TP_{CSD2}-CSD1	TP-CSD2-Fw-EcoRI	CAGAATTCATGGCTGCCACCAACACAATCCT
	TP-CSD2-Rv-NcoI	CACCATGGGAAGCACTGCAACAGCCTTCT
TP_{CSD2}-CSD1	CSD1-Fw-NcoI	TCTCCATGGCGAAAGGAGTTGCAGTTTT

	CSD1-Rv	TTAGCCCTGGAGACCAATGATGC
Full length CSD1-YFP	CSD1-Fw-NcoI	TCTCCATGGCGAAAGGAGTTGCAGTTTT
	CSD1ns-Rv-SalI	CAGTCGACCCGCCCTGGAGACCAATGATG
TP_{CSD2}-CSD1-YFP	CSD1-Fw-NcoI	TCTCCATGGCGAAAGGAGTTGCAGTTTT
	CSD1ns-Rv-SalI	CAGTCGACCCGCCCTGGAGACCAATGATG
GST-CSD1	CSD1-Fw-EcoRI	CAGAATTCATGGCGAAAGGAGTTGCAGT
	CSD1-Rv	TTAGCCCTGGAGACCAATGATGC
Full length CSD3 (and RT-PCR)	CSD3-Fw-EcoRI	TCTGAATTCATGGAAGCTCCTAGAGGAAATCT
	CSD3-Rv-EcoRI	TCTGAATTCCTATAGTTTAGCATCCGCAGATG
CSD3-ΔAKL	CSD3-Fw-EcoRI	TCTGAATTCATGGAAGCTCCTAGAGGAAATCT
	CSD3-Rv-ΔAKL	CACTAATCCGCAGATGATTGAAGTCC
GFP- full length CSD3	CSD3-Fw-SmaI	CACCCGGGCCATGGAAGCTCCTAGAGGAAAT
	CSD3-Rv-EcoRI	TCTGAATTCCTATAGTTTAGCATCCGCAGATG
GFP-CSD3-ΔAKL	CSD3-Fw-SmaI	CACCCGGGCCATGGAAGCTCCTAGAGGAAAT
	CSD3-Rv-ΔAKL	CACTAATCCGCAGATGATTGAAGTCC
ROXY1	ROXY1-Fw-SmaI	CACCCGGGATGCAATACCAGACAGAATC
	ROXY1-Rv-BamHI	CAGGATCCTCAGAGCCAGAGAGCG
GRXcp	GRXcp-Fw-SmaI	CACCCGGGATGGCTCTCCGATCTGTCAAA
	GRXcp-Rv-BamHI	CAGGATCCTCAAGAGCACATAGCTTTCTCCA

APPENDIX

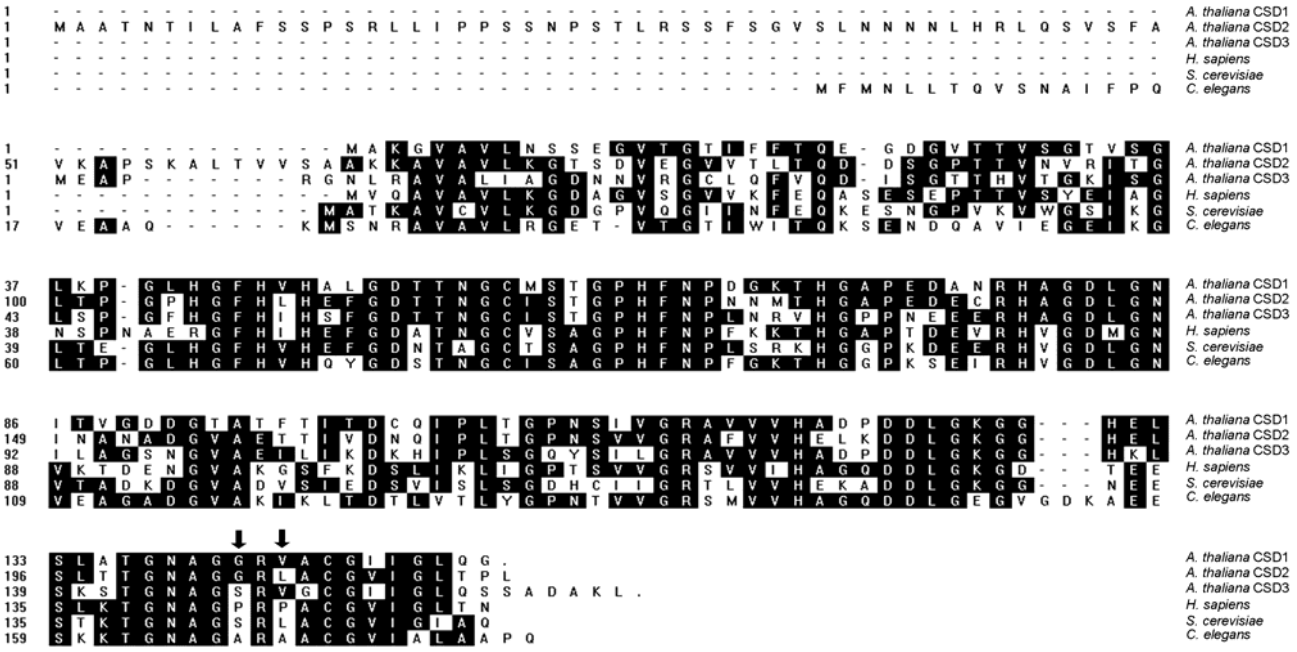

Appendix 1. The alignment of CSD genes in *Arabidopsis*, human, yeast and nemadote.

Arrows indicate position corresponding to residues141 and 143 of CSD1 protein. Identical residues are highlight in black.

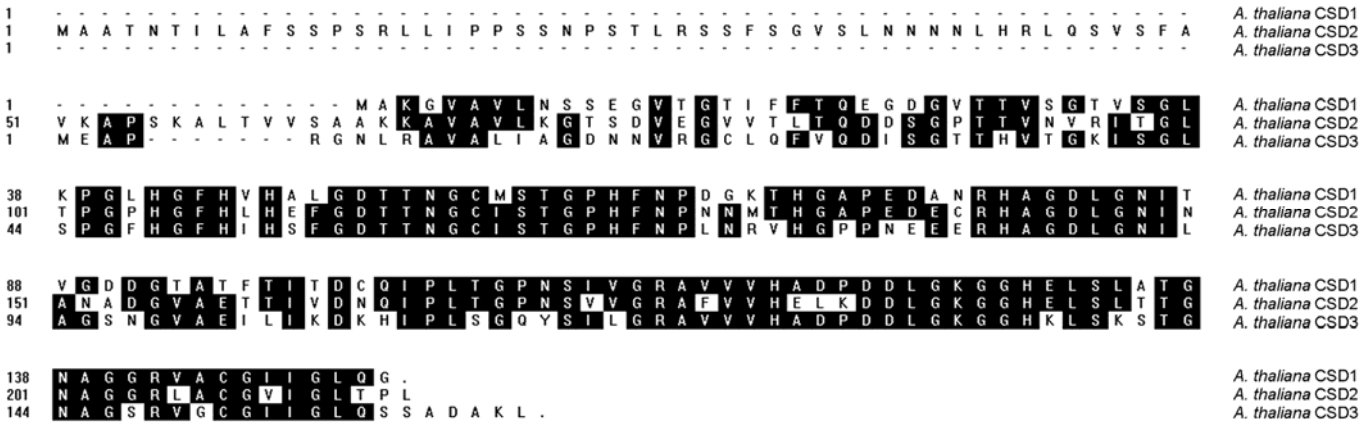

Appendix 2. The alignment of protein sequences of *Arabidopsis* CSD1, CSD2 and CSD3.

Identical residues are highlight in black.

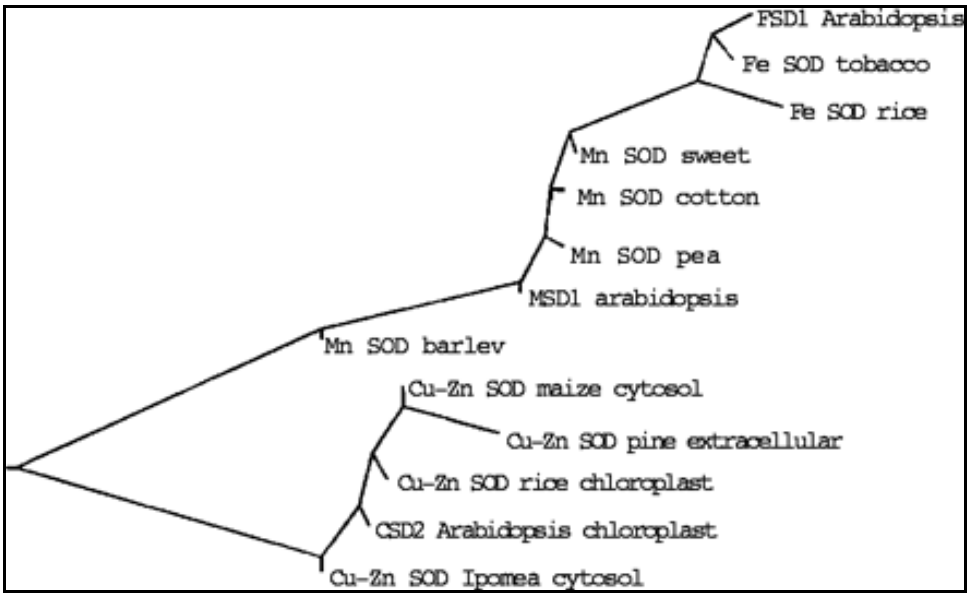

Appendix 3. Relatedness of SOD protein sequences in some plant cells (Alscher et al., 2002)

Transcription factors	CSD1	CSD2	CSD3	FSD1	FSD2	FSD3	MSD1
ABRE	◆					◆	
NF-κB	◆	◆	◆			◆	◆
Heat shock element			◆		◆		◆
Y-box			◆				◆

Appendix 4. A comparison of the upstream regions of the seven *Arabidopsis* SODs (Alscher et al., 2002)

REFERENCES

Abdel-Ghany, S.E., Burkhead, J.L., Gogolin, K.A., Andres-Colas, N., Bodecker, J.R., Puig, S., Penarrubia, L., and Pilon, M. (2005). AtCCS is a functional homolog of the yeast copper chaperone Ccs1/Lys7. FEBS Lett. **579:** 2307-2312.

Abdel-Ghany S.E., Pilon M. (2008). MicroRNA-mediated systemic down-regulation of copper protein expression in response to low copper availability in Arabidopsis. J Biol Chem. **283**:15932-15945.

Alscher, R.G., Erturk, N., and Heath, L.S. (2002). Role of superoxide dismutases (SODs) in controlling oxidative stress in plants. J. Exp. Bot. **53:** 1331-1341.

Ascone, I., Longo, A., Dexpert, H., Ciriolo, M.R., Rotilio, G., and Desideri, A. (1993). An X-ray absorption study of the reconstitution process of bovine Cu,Zn superoxide dismutase by Cu(I)-glutathione complex. FEBS Lett. **322:** 165-167.

Bannister J.V., Parker M.W. (1985). The presence of a copper/zinc superoxide dismutase in the bacterium Photobacterium leiognathi: a likely case of gene transfer from eukaryotes to prokaryotes. PNAS. **82**: 149–152.

Bannister W.H., Bannister J.V., Barra D., Bond J., Bossa F. (1991). Evolutionary aspects of superoxide dismutase: the copper/zinc enzyme. Free Radic Res Commun. **1**:349-361.

Beem K.M., Rich W.E., Rajagopalan K.V. (1974). Total reconstitution of copper-zinc superoxide

dismutase. J Biol Chem. **249**: 7298-7305.

Beyer, W., Imlay, J., and Fridovich, I. (1991). Superoxide dismutases. Prog. Nucleic Acid Res. Mol. Biol. **40:** 221-253.

Borchelt, D.R., Lee, M.K., Slunt, H.S., Guarnieri, M., Xu, Z.S., Wong, P.C., Brown, R.H., Jr., Price, D.L., Sisodia, S.S., and Cleveland, D.W. (1994). Superoxide dismutase 1 with mutations linked to familial amyotrophic lateral sclerosis possesses significant activity. Proc. Natl. Acad. Sci. U S A **91:** 8292-8296.

Bordo D., Djinović K., Bolognesi M. (1994) Conserved patterns in the Cu,Zn superoxide dismutase family. J. Mol. Biol. **238**: 366-386.

Bowler, C., Montagu, M.V., and Inze, D. (1992). Superoxide dismutase and stress tolerance. Annu. Rev. Plant Physiol. Plant Mol. Biol. **43:** 83-116.

Bradford, M.M. (1976). A rapid and sensitive method for the quantitation of microgram quantities of protein utilizing the principle of protein-dye binding. Anal. Biochem. **72:** 248-254.

Brown, N.M., Torres, A.S., Doan, P.E., and O'Halloran, T.V. (2004). Oxygen and the copper chaperone CCS regulate posttranslational activation of Cu,Zn superoxide dismutase. Proc. Natl. Acad. Sci. USA **101:** 5518-5523.

Bueno, P., Varela, J., Gimeenez-Gallego, G., and del Rio, L.A. (1995). Peroxisomal copper, zinc superoxide dismutase: characterization of the isoenzyme from watermelon cotyledons. Plant

Physiol. **108:** 1151-1160.

Burkhead J.L., Reynolds K.A., Abdel-Ghany S.E., Cohu C.M., Pilon M. (2009). Copper homeostasis. New Phytol. Jun. **182**:799-816.

Carroll, M.C., Girouard, J.B., Ulloa, J.L., Subramaniam, J.R., Wong, P.C., Valentine, J.S., and Culotta, V.C. (2004). Mechanisms for activating Cu- and Zn-containing superoxide dismutase in the absence of the CCS Cu chaperone. Proc. Natl. Acad. Sci. USA **101:** 5964-5969.

Carroll, M.C., Outten, C.E., Proescher, J.B., Rosenfeld, L., Watson, W.H., Whitson, L.J., Hart, P.J., Jensen, L.T., and Cizewski Culotta, V. (2006). The effects of glutaredoxin and copper activation pathways on the disulfide and stability of Cu,Zn superoxide dismutase. J. Biol. Chem. **281:** 28648-28656.

Casareno, R.L., Waggoner, D., and Gitlin, J.D. (1998). The copper chaperone CCS directly interacts with copper/zinc superoxide dismutase. J. Biol. Chem. **273:** 23625-23628.

Cheng, N.H., Liu, J.Z., Brock, A., Nelson, R.S., and Hirschi, K.D. (2006). AtGRXcp, an *Arabidopsis* chloroplastic glutaredoxin, is critical for protection against protein oxidative damage. J. Biol. Chem. **281:** 26280-26288.

Choi H., Hong J., Ha J., Kang J., Kim S.Y. (2000). ABFs, a family of ABA-responsive element binding factors. J Biol Chem. **275**: 1723–1730.

Chu, C.C., Lee, W.C., Guo, W.Y., Pan, S.M., Chen, L.J., Li, H.M., and Jinn, T.L. (2005). A copper chaperone for superoxide dismutase that confers three types of copper/zinc superoxide dismutase activity in *Arabidopsis*. Plant Physiol. **139:** 425-436.

Cohu, C.M., Abdel-Ghany, S.E., Gogolin Reynolds, K.A., Onofrio, A.M., Bodecker, J.R., Kimbrel, J.A., Niyogi, K.K., and Pilon, M. (2009). Copper delivery by the copper chaperone for chloroplast and cytosolic copper/zinc-superoxide dismutases: regulation and unexpected phenotypes in an *Arabidopsis* mutant. Mol. Plant **2:** 1336-1350.

Colicelli, J., Birchmeier, C., Michaeli, T., O'Neill, K., Riggs, M., and Wigler, M. (1989). Isolation and characterization of a mammalian gene encoding a high-affinity cAMP phosphodiesterase. Proc. Natl. Acad. Sci. USA **86:** 3599-3603.

Corson, L.B., Strain, J.J., Culotta, V.C., and Cleveland, D.W. (1998). Chaperone-facilitated copper binding is a property common to several classes of familial amyotrophic lateral sclerosis-linked superoxide dismutase mutants. Proc. Natl. Acad. Sci. USA **95:** 6361-6366.

Crapo J.D., Oury T., Rabouille C., Slot J.W., Chang L.Y. (1992). Copper,zinc superoxide dismutase is primarily a cytosolic protein in human cells. Proc. Natl. Acad. Sci. USA. **89**:10405-10409

Culotta, V.C., Klomp, L.W., Strain, J., Casareno, R.L., Krems, B., and Gitlin, J.D. (1997). The copper chaperone for superoxide dismutase. J. Biol. Chem. **272:** 23469-23472.

Dhaunsi G.S., Gulati S., Singh A.K., Orak J.K., Asayama K., Singh I. (1992). Demonstration of Cu-Zn superoxide dismutase in rat liver peroxisomes. Biochemical and immunochemical evidence. J Biol Chem. **267**: 6870-6873.

Dugas D.V., Bartel B. (2008). Sucrose induction of Arabidopsis miR398 represses two Cu/Zn superoxide dismutases. Plant Mol Biol. **67**: 403-417.

Forman, H.J., and Fridovich, I. (1973). On the stability of bovine superoxide dismutase. The effects of metals. J. Biol. Chem. **248:** 2645-2649.

Furukawa, Y., Torres, A.S., and O'Halloran, T.V. (2004). Oxygen-induced maturation of SOD1: a key role for disulfide formation by the copper chaperone CCS. EMBO J. **23:** 2872-2881.

Fridovich I. (1986). Biological effects of the superoxide radical. Arch Biochem Biophys. **247**: 1-11.

Guan L., Scandalios J.G. (1998). Two structurally similar maize cytosolic superoxide dismutase genes, Sod4 and Sod4A, respond differentially to abscisic acid and high osmoticum. Plant Physiol. **117**: 217–224.

Gutteridge J.M., Halliwell B. (1989). Iron toxicity and oxygen radicals. Baillieres Clin Haematol. **2**:195-256.

Halliwell, B., and Gutteridge, J.M.C. (1999). Free Radicals in Biology and Medicine. 3rd ed. (Oxford: Clarendon Press).

Hancock, K.R., Phillips, L.D., White, D.W., and Ealing, P.M. (1997). pPE1000: a versatile

vector for the expression of epitope-tagged foreign proteins in transgenic plants. Biotechniques **22:** 861-865.

Jackson, C., Dench, J., Moore, A.L., Halliwell, B., Foyer, C.H., and Hall, D.O. (1978). Subcellular localisation and identification of superoxide dismutase in the leaves of higher plants. Eur. J. Biochem. **91:** 339-344.

Jensen, L.T., and Culotta, V.C. (2005). Activation of CuZn superoxide dismutases from Caenorhabditis elegans does not require the copper chaperone CCS. J. Biol. Chem. **280:** 41373-1379.

Kanematsu, S., and Asada, K. (1989). CuZn-superoxide dismutase in rice: occurrence of an active, monomeric enzyme and two types of isozyme in leaf and non-photosynthetic tissues. Plant Cell Physiol. **30:** 381-391.

Kanematsu, S., and Asada, K. (1990). Characteristic Amino Acid Sequences of Chloroplast and Cytosol Isozymes of CuZn-Superoxide Dismutase in Spinach, Rice and Horsetail. Plant Cell Physiol. **31:** 99-112.

Kliebenstein, D.J., Monde, R.A., and Last, R.L. (1998). Superoxide dismutase in *Arabidopsis*: an eclectic enzyme family with disparate regulation and protein localization. Plant Physiol. **118:** 637-650.

Kropat J., Tottey S., Birkenbihl R.P., Depège N., Huijser P., Merchant S. (2005). A regulator of

nutritional copper signaling in Chlamydomonas is an SBP domain protein that recognizes the GTAC core of copper response element. Proc Natl Acad Sci. **102**: 18730-18735.

Lamb, A.L., Torres, A.S., O'Halloran, T.V., and Rosenzweig, A.C. (2001). Heterodimeric structure of superoxide dismutase in complex with its metallochaperone. Nat. Struct. Biol. **8:** 751-755.

Lee, Y.J., Kim, D.H., Kim, Y.W., and Hwang, I. (2001). Identification of a signal that distinguishes between the chloroplast outer envelope membrane and the endomembrane system in vivo. Plant Cell **13:** 2175-2190.

Leitch, J.M., Jensen, L.T., Bouldin, S.D., Outten, C.E., Hart, P.J., and Culotta, V.C. (2009a). Activation of Cu,Zn-superoxide dismutase in the absence of oxygen and the copper chaperone CCS. J. Biol. Chem. **284:** 21863-21871.

Leitch, J.M., Yick, P.J., and Culotta, V.C. (2009b). The right to choose: multiple pathways for activating copper,zinc superoxide dismutase. J. Biol. Chem. **284:** 24679-24683.

Leunissen J.A.M., de Jong W.W. (1986). Copper/zinc superoxide dismutase: how likely is gene transfer from ponyfish to Photobacter leiognathi? J. of Mole. Evol. **23**: 250–258.

Lepock, J.R., Arnold, L.D., Petkau, A., and Kelly, K. (1981). Interaction of superoxide dismutase with phospholipid liposomes. An uptake, spin label and calorimetric study. Biochim. Biophys. Acta **649:** 45-57.

Lockwood T.D. (2003). Redox pacing of proteome turnover: influences of glutathione and ketonemia. Arch. Biochem. Biophys. **417:** 183-193.

Martin J.P., Fridovich I. (1981). Evidence for a natural gene transfer from the ponyfish to its bioluminescent bacterial symbiont Photobacter leiognathi. The close relationship between bacteriocuprein and the copper-zinc superoxide dismutase of teleost fishes. J. Biol. Chem. **256**: 6080–6089.

Marres C.A., Van Loon A.P., Oudshoorn P., Van Steeg H., Grivell L.A., Slater E.C. (1985). Nucleotide sequence analysis of the nuclear gene coding for manganese superoxide dismutase of yeast mitochondria, a gene previously assumed to code for the Rieske iron-sulphur protein. Eur J Biochem. **147**:153-161

McCord, J.M., and Fridovich, I. (1969). Superoxide dismutase: an enzymic function for erythrocuprein (hemocuprein). J. Biol. Chem. **244:** 6049-6055.

Myouga F., Hosoda C., Umezawa T., Iizumi H., Kuromori T., Motohashi R., Shono Y., Nagata N., Ikeuchi M., Shinozaki K. (2008). A heterocomplex of iron superoxide dismutases defends chloroplast nucleoids against oxidative stress and is essential for chloroplast development in Arabidopsis. Plant Cell. **20**:3148-3162

Pasternak, M., Lim, B., Wirtz, M., Hell, R., Cobbett, C.S., and Meyer, A.J. (2008). Restricting glutathione biosynthesis to the cytosol is sufficient for normal plant development. Plant J. **53:**

999-1012.

Rae, T.D.,Schmidt, P. J., Pufahl, R.A., Culotta. V. C., and O'Halloran, T. V. (1999). Undetectable intracellular free copper: the requirement of a copper chaperone for superoxide sismutase. Science. **284:** 805-808

Rouhier, N. (2010). Plant glutaredoxins: pivotal players in redox biology and iron-sulphur centre assembly. New Phytol. **186:** 365-372.

Sánchez-Fernández R., Avalos J., Cerdá-Olmedo E. (1997). Inhibition of gibberellin biosynthesis by nitrate in Gibberella fujikuroi. FEBS Lett. **413**:35-39

Sandalio L.M., Del Río L.A. (1988). Intraorganellar distribution of superoxide dismutase in plant peroxisomes (glyoxysomes and leaf peroxisomes). Plant Physiol. **88**:1215-1218.

Santos M., Gousseau H., Lister C., Foyer C., Creissen G., Mullineaux P. (1996). Cytosolic ascorbate peroxidase from Arabidopsis thaliana L. is encoded by a small multigene family. Planta. **198**: 64–69.

Schmidt, P. J., Rae, T. D., Pufahl, R. A., Hamma, T., Strain, J., O' Halloran, T. V., and Culotta, V. C. (1999) Multiple protein domains contribute to the action of the copper chaperone for superoxide dismutase. J. Biol. Chem. **274:** 23719 – 23725

Shcolnick S., Keren N. (2006). Metal homeostasis in cyanobacteria and chloroplasts. Balancing benefits and risks to the photosynthetic apparatus. Plant Physiol. **141**:805-810.

Smith, M.W., and Doolittle, R.F. (1992) A comparison of evolutionary rates of the two major kinds of superoxide dismutase. J. Mol. Evol. **34**: 175-84

Subramaniam, J.R., Lyons, W.E., Liu, J., Bartnikas, T.B., Rothstein, J., Price, D.L., Cleveland, D.W., Gitlin, J.D., and Wong, P.C. (2002). Mutant SOD1 causes motor neuron disease independent of copper chaperone-mediated copper loading. Nat. Neurosci. **5:** 301-307.

Sunkar R., Kapoor A., Zhu J.K. (2006). Posttranscriptional induction of two Cu/Zn superoxide dismutase genes in Arabidopsis is mediated by downregulation of miR398 and important for oxidative stress tolerance. Plant Cell. **18**: 2051-2065.

Steinman H.M. (1982). Copper-zinc superoxide dismutase from Caulobacter crescentus CB15. A novel bacteriocuprein form of the enzyme. J. Biol. Chem. **257**:10283–10293.

Steinman H.M. (1985). Bacteriocuprein superoxide dismutases in pseudomonads. J. of Bacte. **162**: 1255–1260.

Takahashi, M.A., and Asada, K. (1983). Superoxide anion permeability of phospholipid membranes and chloroplast thylakoids. Arch. Biochem. Biophys. **226:** 558-566.

Valentine J.S., Gralla E.B. (1997). Delivering copper inside yeast and human cells. Science. **278:** 817-818.

Wallace, M.A., Liou, L.L., Martins, J., Clement, M.H., Bailey, S., Longo, V.D., Valentine, J.S., and Gralla, E.B. (2004). Superoxide inhibits 4Fe-4S cluster enzymes involved in amino acid

biosynthesis. Cross-compartment protection by CuZn-superoxide dismutase. J. Biol. Chem. **279:** 32055-32062.

Wang, J., Slunt, H., Gonzales, V., Fromholt, D., Coonfield, M., Copeland, N.G., Jenkins, N.A., and Borchelt, D.R. (2003). Copper-binding-site-null SOD1 causes ALS in transgenic mice: aggregates of non-native SOD1 delineate a common feature. Hum. Mol. Genet. **12:** 2753-2764.

Weigel M., Varotto C., Pesaresi P., Finazzi G., Rappaport F., Salamini F., Leister D. (2003). Plastocyanin is indispensable for photosynthetic electron flow in Arabidopsis thaliana. J Biol Chem. **278**: 31286-31289.

Weisiger R.A., Fridovich I. (1973). Mitochondrial superoxide simutase. Site of synthesis and intramitochondrial localization. J Biol Chem. **248**:4793-4796.

Wong, P.C., Waggoner, D., Subramaniam, J.R., Tessarollo, L., Bartnikas, T.B., Culotta, V.C., Price, D.L., Rothstein, J., and Gitlin, J.D. (2000). Copper chaperone for superoxide dismutase is essential to activate mammalian Cu/Zn superoxide dismutase. Proc. Natl. Acad. Sci. USA **97:** 2886-2891.

Xiang, C., Werner, B.L., Christensen, E.M., and Oliver, D.J. (2001). The biological functions of glutathione revisited in *Arabidopsis* transgenic plants with altered glutathione levels. Plant Physiol. **126:** 564-574.

Xing, S., Rosso, M.G., and Zachgo, S. (2005). ROXY1, a member of the plant glutaredoxin family, is required for petal development in *Arabidopsis* thaliana. Development **132:** 1555-1565.

Yamasaki H., Abdel-Ghany S.E., Cohu C.M., Kobayashi Y., Shikanai T., Pilon M. (2007). Regulation of copper homeostasis by micro-RNA in Arabidopsis. J Biol Chem. **282**: 16369-16378.

Yamasaki H., Hayashi M., Fukazawa M., Kobayashi Y., Shikanai T. (2009). SQUAMOSA Promoter Binding Protein-Like7 Is a Central Regulator for Copper Homeostasis in Arabidopsis. Plant Cell. **21**: 347-361.

Yang, P., Fu, H., Walker, J., Papa, C.M., Smalle, J., Ju, Y.M., and Vierstra, R.D. (2004). Purification of the *Arabidopsis* 26 S proteasome: biochemical and molecular analyses revealed the presence of multiple isoforms. J. Biol. Chem. **279:** 6401-6413.

Yoo, S.D., Cho, Y.H., and Sheen, J. (2007). *Arabidopsis* mesophyll protoplasts: a versatile cell system for transient gene expression analysis. Nat. Protoc. **2:** 1565-1572.

Zelkó R., Süvegh K. (2002). Influence of storage conditions on the physical aging of amorphous polyvinylpyrrolidone. Acta Pharm Hung. **72**:123-126.